DEVELOPMENT OF LABORATORY TEST METHOD TO REPLACE THE SIMULATED HIGH-TEMPERATURE FLUIDITY TEST

By

ALEXANDER DEREK PIPER

A THESIS PRESENTED TO THE GRADUATE SCHOOL
OF THE UNIVERSITY OF FLORIDA IN PARTIAL FULFILLMENT
OF THE REQUIREMENTS FOR THE DEGREE OF
MASTER OF SCIENCE

UNIVERSITY OF FLORIDA
2012

ACKNOWLEDGEMENTS

The author would like to thank Florida Department of Transportation (FDOT) State Materials Office and Structural Laboratory for their support during testing. This project would not be possible without the help of Mike Bergin, Patrick Carlton, Mark Conley, Dale DeFord, Richard DeLorenzo, Toby Dillow, Joseph Fitzgerald, Thomas Frank, Charles Ishee, Kingsley Lau, Mario Paredes, Richard Nalli III, Jordan Nelson, Teresa Risher, and Duane Robertson.

The author also would also like to thank his supervisory committee at the University of Florida: Trey Hamilton, Christopher Ferraro, and Mang Tia. University of Florida students Sai Jiang, Garrett Littlejohn, Kyle Mays, Alex Randell, Philip Strauss, Michael Willis, and Zack Workman are thanked for their assistance with testing. The author would like to thank Eshan Dave, Andrea Schokker, and Andrew Venaas at the University of Minnesota for their contributions. Clarissa Ferraris provided a great deal of insight into the rheological research. Additionally, John Newton shared his expertise on grouting.

TABLE OF CONTENTS

Page

ACKNOWLEDGEMENTS 3

LIST OF TABLES 6

LIST OF FIGURES 7

LIST OF DEFINITIONS 11

ABSTRACT 14

CHAPTER

1 INTRODUCTION 16

2 LITERATURE REVIEW 18

2.1 Post-Tensioning Grouts 18
2.2 High-Temperature Grout Fluidity Test 20
2.3 Definition and Properties of a Suspension 20
2.4 Rheology Introduction 21
2.5 Rheology Equipment 22
2.6 Rheology Theory 23
2.7 DSR Testing of Grout 27
2.8 DSR Geometry 30
2.9 Relationship between Flow Cone and Rheology 31
2.10 Shear Rates Imposed by Field Equipment 32

3 APPROACH 33

4 MATERIALS 35

5 MIXING AND AGITATION EQUIPMENT 36

5.1 Colloidal Grout Plant 36
5.2 High Shear Mixer 40
5.3 Blender Mixer 43

6 DYNAMIC SHEAR RHEOMETER EQUIPMENT 47

6.1 DSR Geometries 48
6.1.1 Serrated Parallel Plates 48
6.1.2 Cup and Ribbon 49
6.2 Cup and Ribbon Geometry Calibration 51
6.2.1 Reference Material 52
6.2.2 DSR Calibration Results 54

6.3 DSR Geometry Selection 60

7 REVIEW OF CURRENTLY AVAILABLE DSR TEST METHODS 62

7.1 Testing Shear Rates 62
7.2 Flow Curve Test 63
7.3 Stress Growth Test 66
7.4 Oscillatory Time Sweep Test 69

8 APPARENT VISCOSITY TEST 74

8.1 Testing Shear Rate 75
8.2 Testing Time 81
8.3 Summary 84

9 HIGH TEMPERATURE GROUT FLUIDITY TEST 85

9.1 Flow Cone Test 89
9.2 Mud Balance Test 90
9.3 Unit Weight Test 91

10 RESULTS AND DISCUSSION – HIGH TEMPERATURE GROUT FLUIDITY TEST 94

10.1 Flow Cone Test Results 94
10.2 Apparent Viscosity Test Results 95
10.3 Temperature Results 96
10.4 Pressure and Flow Rate Results 97
10.5 Mud Balance and Unit Weight Results 99

11 FLOW CONE TO APPARENT VISCOSITY CALIBRATION 101

12 DEVELOPMENT OF SIMULATED CONDITIONING TECHNIQUE 104

12.1 Temperature 104
12.2 DSR Conditioning 106
12.3 High Shear Mixer Conditioning 109

13 SUMMARY AND CONCLUSIONS 113

14 RECOMMENDATIONS 116

LIST OF REFERENCES 118

BIOGRAPHICAL SKETCH 121

LIST OF TABLES

Table Page

5-1 Comparison of mixing volume for each mixer. 36

6-1 Summary of measured Bingham standard material values. 58

7-1 Summary of shear rates imposed by flow cone nozzle. 63

7-2 Summary of LVR for each type of grout. 72

8-1 Summary of R^2 values for linear trend-line fit to apparent viscosity versus flow cone time results at different shear rates. 80

10-1 Summary of ambient and grout temperatures measured during HTGF test. 97

10-2 Summary of initial unit weights as well as maximum increase and decrease in unit weight during testing. 100

11-1 Recommended criteria for qualifying grouts using apparent viscosity test. 102

12-1 Comparison of apparent viscosity results under different conditioning techniques. 108

12-2 Recommended criteria for qualifying grouts using high shear mixer and flow cone. 111

14-1 Recommended criteria for qualifying grouts using apparent viscosity test. 116

14-2 Recommended criteria for qualifying grouts using high shear mixer and flow cone. 117

LIST OF FIGURES

Figure Page

2-1 Precast concrete bridge segment with PT ducts and tendons shown..... 18

2-2 Flow cone used to determine rheological properties of grout in the field 19

2-3 Parallel plate rheometer geometry..... 22

2-4 Simple stress-strain model for steel..... 23

2-5 Flow curve for Newtonian fluid model..... 24

2-6 Flow curves for several non-Newtonian fluid models..... 24

2-7 Thixotropic effects observed in material subjected to constant shear rate over a period of time..... 26

3-1 Flow chart depicting research approach..... 34

5-1 Chemgrout CG600 13 c.f. colloidal grout plant with various parts labeled..... 37

5-2 375-cfm diesel air compressor used to power grout plant. 37

5-3 Add water to mix tank. 38

5-4 Add one bag of grout at a time. 39

5-5 Continue running colloidal mixer and agitator paddle for 2 minutes after adding last bag of grout. 39

5-6 Pump grout to target..... 40

5-7 High shear mixer used to prepare grout samples 41

5-8 Pour water into the mix tank 42

5-9 Add dry material to mixer over a period of 3-5 minutes 42

5-10 Raise mixer head and scrape low speed agitator paddle. 43

5-11 Waring HGBTAC30 commercial blender used for mixing..... 44

5-12 Blade configuration used in mix procedure with quarter shown for reference 44

5-13 Plunger mixer used to agitate grout before testing 46

6-1 TA AR2000ex Dynamic Shear Rheometer with helical ribbon and cup geometry 47

6-2 Serrated parallel plate DSR geometry 48

6-3 Helical ribbon and cup DSR geometry..... 50

6-4 Dimensions of helical ribbon and cup DSR geometry..... 50

6-5 Flow curve for Bingham plastic material. 53

6-6 NIST certified Bingham yield stress values with respect to time after mixing. 54

6-7 NIST certified Bingham plastic viscosity values with respect to time after mixing. 54

6-8 Flow curve results for SRM on the same day as mixing. 55

6-9 Ratio of certified Bingham yield stress to measured Bingham yield stress with respect to time after mixing for batch prepared with tap water. 56

6-10 Ratio of certified Bingham yield stress to measured Bingham yield stress with respect to time after mixing for batch prepared with distilled water. 56

6-11 Ratio of certified Bingham plastic viscosity to measured Bingham yield stress with respect to time after mixing for batch prepared with tap water. 57

6-12 Ratio of certified Bingham plastic viscosity to measured Bingham yield stress with respect to time after mixing for batch prepared with distilled water. 57

6-13 Variation in adjusted Bingham yield stress with respect to time after mixing. 59

6-14 Variation in adjusted Bingham plastic viscosity with respect to time after mixing. 59

7-1 Flow curve for grout C40, 21 minutes after mixing. 64

7-2 Flow curve for materials PT1-3, PT2-3, PT3-2, and PT4-3..... 65

7-3 Idealized plot of stress growth test showing yield point. 67

7-4 Plot of shear stress vs. time for grout C45. Tested using cup and ribbon with shear rate of 0.1 s^{-1}. 68

7-5 Plot of shear stress vs. time for grout PT1-1. Tested using cup and ribbon with shear rate of 0.1 s^{-1}. 68

7-6 Plot of G' and G" vs. strain for grout C45..... 71

7-7 Plot of G' and G" vs. strain for grout PT1-1. 71

7-8 Plot of G' and G" vs. strain for grout PT2-1. 72

7-9 Plot of storage modulus vs. time for all tested grouts. 73

8-1 Plot of DSR viscosity versus flow cone time for DSR testing shear rate of 5 s^{-1}. 77

8-2 Plot of DSR viscosity versus flow cone time for DSR testing shear rate of 25 s^{-1}. 77

8-3 Plot of DSR viscosity versus flow cone time for DSR testing shear rate of 50 s^{-1}. 78

8-4 Plot of DSR viscosity versus flow cone time for DSR testing shear rate of 75 s^{-1}. 78

8-5 Plot of DSR viscosity versus flow cone time for DSR testing shear rate of 100 s^{-1}. 79

8-6 Plot of DSR viscosity versus flow cone time for DSR testing shear rate of 165 s^{-1}..... 79

8-7 Results of 60-minute apparent viscosity test conducted on grouts C45, PT1-1, PT2-1, PT3-1, and PT4-1. 82

8-8 Results of first 5 minutes of apparent viscosity test conducted on grouts C45, PT1-1, PT2-1, PT3-1, and PT4-1..... 83

9-1 Environmental chamber used for temperature control during HTGF testing..... 86

9-2 Inside of environmental chamber used for temperature control during HTGF 86

9-3 Transfer grout to agitation tank and start agitator paddle 87

9-4 Return grout to agitation tank after pumping through 400 ft. of hose..... 87

9-5 Collect 2-3 gallon sample from return end of 400 ft. of hose into 5-gallon bucket..... 88

9-6 Paint paddle style agitator used to shear grout within 10 seconds of flow cone testing 89

9-7 Flow cone used to determine fluidity of grout samples during HTGF testing..... 90

9-8 Mud balance used to determine unit weight of grout samples during HTGF testing..... 91

9-9 Unit weight used to determine grout density..... 92

9-10 Unit weight being filled for testing 92

10-1 Plot of flow cone results versus recirculation time for all HTGF tests. 94

10-2 Plot of DSR apparent viscosity versus recirculation time for all HTGF tests..... 95

10-3 Plot of ambient temperature and grout temperature versus recirculation time for all grouts tested in HTGF test..... 96

10-4 Plot of pumping pressure and grout flow rate versus recirculation time for all grouts tested in HTGF test. 98

10-5 Plot of mud balance density and unit weight versus recirculation time for all grouts tested in HTGF test. 99

11-1 Plot of apparent viscosity versus flow cone time for samples collected during HTGF test..... 101

11-2 Apparent viscosity results from HTGF test with failure limits shown..... 103

12-1 Plot of apparent viscosity vs. time after mixing for grout C45 at different temperatures with no conditioning between tests..... 105

12-2 Plot of apparent viscosity vs. time after mixing for grout PT1-1 at different temperatures with no conditioning between tests..... 105

12-3 Plot of apparent viscosity vs. time after mixing for grout PT2-1 at different temperatures. 106

12-4 Plot of apparent viscosity measured when DSR was used for grout conditioning versus apparent viscosity measured during HTGF test..... 107

12-5 Plot of flow cone time measured where high shear mixer was used for grout conditioning versus flow cone time measured during HTGF test..... 110

12-6 Selected data from plot of flow cone time measured where high shear mixer was used for grout conditioning versus flow cone time measured during HTGF test..... 111

12-7 Plot of mud balance value measured where high shear mixer was used for grout conditioning versus mud balance value measured during HTGF test. 112

LIST OF DEFINITIONS

Definitions are from Hackley and Ferraris (2001), unless otherwise noted.

ANTI-THIXOTROPY	A reversible time-dependent increase in viscosity at a particular shear rate. Shearing causes a gradual growth in structure over time. See Figure 2-7.
APPARENT VISCOSITY	The value of viscosity evaluated at some nominal shear rate.
COLLOID	A substance that is in a state of division preventing passage through a semipermeable membrane, consisting of particles ranging from 0.1 to 0.001 µm in diameter. (ACI 2010)
COLLOIDAL GROUT	Grout in which a substantial proportion of the solid particles have the size range of a colloid. (ACI 2010)
COLLOIDAL MIXER	A mixer designed to produce colloidal grout (ACI 2010). Grout mixer used to disperse cementitious material down to its finest particle size to achieve complete particle wetness (ChemGrout).
FLOW CURVE	A graphical representation of the behavior of flowing materials in which shear stress is related to shear rate. See Figure 2-4 and Figure 2-6.
FLOW CURVE TEST	A DSR test in which a linearly-increasing shear rate is imposed on a material. Shear stress is measured and plotted against shear rate to generate a flow curve.
GROUT	A mixture of cementitious material and water, with or without aggregate, proportioned to produce a pourable consistency without segregation of the constituents; also a mixture of other composition but of similar consistency. (ACI 2010)
LOSS MODULUS	The out-of-phase (viscous) component of oscillatory flow (Hackley and Ferraris 2001). The liquid-like component of a material measured using an oscillatory test (Barnes 2000).
NEWTONIAN FLUID	Flow model of fluids in which a linear relationship exists between shear stress and shear rate, where the coefficient of viscosity is the constant of proportionality. See Figure 2-5.

NON-NEWTONIAN FLUID	Flow model of fluids that are not characterized by a linear relationship between shear stress and shear rate.
PLAIN GROUT	A grout composed of portland cement and water only.
POST-TENSIONING	Method of prestressing in which prestressing steel is tensioned after concrete has hardened. (ACI 2010)
POST-TENSIONING, BONDED	Post-tensioned construction in which the annular spaces around the tendons are grouted after stressing, thereby bonding the tendon to the concrete section. (ACI 2010)
PT GROUT	A colloidal grout composed of portland cement, water, and other additives intended to improve fluid and hardened properties.
SHEAR RATE	The rate of change of shear strain with time. For liquids, the shear rate, rather than strain, is generally used in describing flow.
SHEAR STRESS	The component of stress that causes successive parallel layers of a material body to move, in their own planes (i.e., the plane of shear), relative to each other.
SHEAR THICKENING	An increase in viscosity with increasing shear rate during steady shear flow. See Figure 2-6.
SHEAR THINNING	A decrease in viscosity with increasing shear rate during steady shear flow. See Figure 2-6.
STORAGE MODULUS	The in-phase (elastic) component of oscillatory flow (Hackley and Ferraris 2001). The solid-like component of a material measured using an oscillatory test. (Barnes 2000).
STRESS GROWTH	When an instantaneous and constant strain (or shear rate) is applied to a material while stress is measured over time, an increasing stress vs. time or modulus vs. time function is termed stress growth.
STRUCTURE	In rheology, structure is a term that refers to the formation of stable physical bonds between particles (or chemical bonds between macromolecules) in a fluid. These bonds result in aggregate, floc, or network structure, which impacts the rheological behavior of the fluid and provides elastic and plastic properties. The term may be extended to include structural effects caused by electroviscous interactions, physical bonds between polymers (e.g., associative thickeners), shear-induced alignment of

	anisotropic particles, and close-packing (radial distribution) correlations in concentrated suspensions. The term "structure" is commonly invoked even when little is known about the cause of observed changes in rheological properties.
THIXOTROPY	A reversible time-dependent decrease in viscosity at a particular shear rate. Shearing causes a gradual breakdown in structure over time. See Figure 2-7.
VISCOPLASTIC	A hybrid property in which a material behaves like a solid below some critical stress value, the yield stress, but flows like a viscous liquid when this stress is exceeded. Often associated with highly aggregated suspensions and polymeric gels. See Figure 2-6.
VISCOSITY	The tendency of a liquid to resist flow as a result of internal friction. During viscous flow, mechanical energy is dissipated as heat and the stress that depends on the rate of deformation. Viscosity is the ratio of shear stress to shear rate.
YIELD STRESS	A critical shear stress value below which an ideal plastic or viscoplastic material behaves like a solid (i.e., will not flow). Once the yield stress is exceeded, a viscoplastic material flows like a liquid. See Figure 2-6.

Abstract of Thesis Presented to the Graduate School
of the University of Florida in Partial Fulfillment of the
Requirements for the Degree of Master of Science

DEVELOPMENT OF LABORATORY TEST METHOD TO REPLACE THE SIMULATED HIGH-TEMPERATURE FLUIDITY TEST

By

Alexander Derek Piper

December 2012

Chair: Trey Hamilton
Major: Civil Engineering

This report contains a summary of the research performed to develop a replacement for the high temperature grout fluidity (HTGF) test. The HTGF test was used in the past by FDOT to qualify post-tensioning (PT) grouts for use in post-tensioned bridge construction. The HTGF test is expensive and cumbersome to run in a typical construction materials testing laboratory. The test requires production-oriented equipment and a temperature-controlled environment for testing.

This research project aimed to develop a replacement for the HTGF test using a dynamic shear rheometer (DSR). The DSR is a complex piece of laboratory equipment that is used to assess the rheological properties of fluid materials. Research using a DSR has been performed on plain grouts in the past in a limited manner.

Several steps were taken to develop a replacement for the HTGF test using a DSR. Two DSR geometries were investigated for their suitability to test PT grout. Currently available DSR test methods were reviewed as well. Ultimately a new DSR test method was developed. The test is run by continuously shearing the material in the DSR for 60 minutes. The new DSR test provides a good alternative to the HTGF test.

In addition to the rheological research, the HTGF test was run multiple times on four commercial PT grouts that are currently on the FDOT qualified products list (QPL). Additionally, an alternative test was developed that allows grouts to be qualified without a DSR or the HTGF test.

CHAPTER 1
INTRODUCTION

This report contains a summary of the research performed to develop a replacement for the high temperature grout fluidity (HTGF) test. The HTGF test was used in the past by FDOT to qualify post-tensioning (PT) grouts for use in post-tensioned bridge construction. The test is run by pumping a batch of grout through 400 feet of hose in a 90°F environment continuously for 60 minutes. The HTGF test is expensive and cumbersome to run in a typical construction materials testing laboratory. The HTGF test was previously a requirement for FDOT's qualified products list (QPL) (FDOT 2007). FDOT does not have the capabilities on a production level to run the HTGF test, making it impossible to assess the fluid properties of PT grouts at high temperature. For this reason, the test has been removed from FDOT's bridge construction specifications (FDOT 2013).

This research project aimed to develop a replacement for the HTGF test using a dynamic shear rheometer (DSR). The DSR is a complex piece of laboratory equipment that is used to assess the properties of fluid materials. FDOT has a DSR at their State Materials Office. Research using a DSR has been performed on grouts in the past in a limited manner. Another objective of this project was to run several HTGF tests simultaneously with DSR tests on four commercial PT grouts that are currently on the FDOT qualified products list (QPL).

To develop a replacement for the HTGF test using a DSR, previous work on DSR testing of grouts was reviewed. Several DSR geometries were investigated for their suitability to test PT grout. Existing test methods were reviewed and performed. Ultimately a new DSR test method was developed which was well-suited for PT grouts.

In addition to the rheological research, the HTGF test was run multiple times on each of the PT grouts. Several mixers including a small scale laboratory mixer, a 10 gallon high shear mixer, and a 13 c.f. colloidal mixer were investigated while running tests. These mixers were investigated for their ability to mix PT grouts at a high rate of shear.

CHAPTER 2
LITERATURE REVIEW

2.1 Post-Tensioning Grouts

Post-Tensioning (PT) grouts are composed primarily of portland cement and water. Prepackaged proprietary grouts may contain such supplementary cementitious materials (SCM) as silica fume, fly ash, or others along with admixtures to improve the fluid and hardened properties of the finished grout. PT grouts are used to fill ducts in precast concrete bridge sections.

Figure 2-1 shows a precast concrete bridge section with PT ducts and tendons visible. The tendons are used to carry the tensile stresses in the bridge. The PT grout fills the cavities between the tendons and the wall of the duct. It also fills the cavities between the individual tendons. This creates a bond between the PT tendon and the precast concrete section in addition to providing corrosion protection for the PT tendon.

Figure 2-1. Precast concrete bridge segment with PT ducts and tendons shown. Photo courtesy of Trey Hamilton.

When the PT grouts are pumped into the ducts they must remain fluid enough to flow past the tendons, but they also must not segregate or bleed before they set. Thick grout causes excessive pumping pressures, which may in turn damage the pumping equipment. Bleed water prevents a complete bond of the tendon to the wall of the duct, and can cause the tendons to corrode. Consequently, the rheological behavior of the grout is very important. The rheological properties are measured in the field using a modified flow cone test during mixing to ensure that the grout has adequate fluidity. A flow cone is shown in Figure 2-2.

(a)

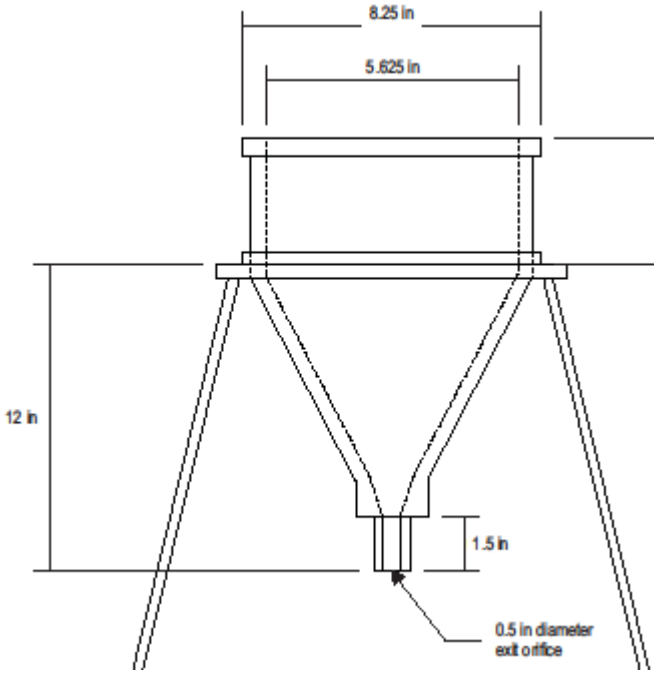

(b)

Figure 2-2. Flow cone used to determine rheological properties of grout in the field (a) and dimensions (b). Photo courtesy of Alex Piper.

2.2 High-Temperature Grout Fluidity Test

The High Temperature Grout Fluidity (HTGF) test was used in the past by FDOT to determine whether or not a grout would remain pumpable under simulated hot weather conditions. The FDOT (2007) bridge construction specifications provided a procedure for running the HTGF test. However, in the FDOT (2013) specifications, the test was removed from the specifications.

2.3 Definition and Properties of a Suspension

A suspension is composed of a discrete number of rigid elements immersed in an interstitial fluid. (Coussout 2005) In the case of a plain cement grout, the cement particles are the elements and water is the interstitial fluid. PT grouts typically behave as suspensions. The use of mineral additives may affect the behavior of the suspension in the case of the PT grouts because the additives can have varying particle sizes.

As the ratio of the volume of the particles to the volume of the fluid increases, the viscosity of the suspension increases. This occurs because the rigid particles displace some of the fluid particles, rendering them unable to flow. Grouts exhibit this behavior as the cement particles hydrate and grow in size. In addition, a number of different internal forces, such as colloidal forces, van der Waals forces, and electrostatic forces, exist between the individual particles in the suspension. As the number of particles increases, the magnitudes of these internal forces also increase; this leads to a further increase in the viscosity of the suspension. (Coussout 2005)

Coussot (2005) states that increasing the number of particles in the suspension also determines whether or not the suspension will behave in a non-Newtonian manner. As long as the particles are dispersed in an isotropic manner, the suspension will exhibit Newtonian behavior. If the particles are not dispersed in an isotropic manner, the

suspension exhibits non-Newtonian properties. An example of this is when the viscosity of the suspension becomes un-proportional to the viscosity of the interstitial fluid. As more particles of varying sizes are added to the suspension, which is the case with PT grouts, it becomes less likely that they will disperse in an isotropic manner. This causes the suspension to become non-Newtonian because the linearity in the flow curve is lost.

Coussout (2005) also states that a structure parameter is often used to describe a suspension. Essentially this parameter is a number between zero and one that can be used to represent the number of internal bonds between particles. A simple model describes de-structuring as the breakage in these bonds due to flow whereas re-structuring is the tendency of the system to return to its equilibrium configuration.

2.4 Rheology Introduction

Rheology is defined as the study of the flow and deformation of materials. Rheology is used to study materials in a wide range of industries from pharmaceuticals to construction materials, as it is in this research project. (Barnes 2000)

Simple fluid materials, such as water, exhibit the same viscosity at any level of applied shear. These materials are called Newtonian fluids. More complex fluids exhibit different viscosities at different levels of applied shear. These materials are called non-Newtonian fluids. (Barnes 2000) An example of a non-Newtonian fluid is toothpaste. If a tube of toothpaste is held upside down, with the lid removed, the toothpaste is extremely viscous and does not flow out of the nozzle. However, when shear is applied to the toothpaste in the form of squeezing, the material flows out of the nozzle.

2.5 Rheology Equipment

A rheometer is used to study the rheological properties of fluid materials. A basic rheometer works by shearing a fluid between two parallel planes. (Hackley and Ferraris 2001) A common rheometer geometry is made up from two parallel plates (Figure 2-3).

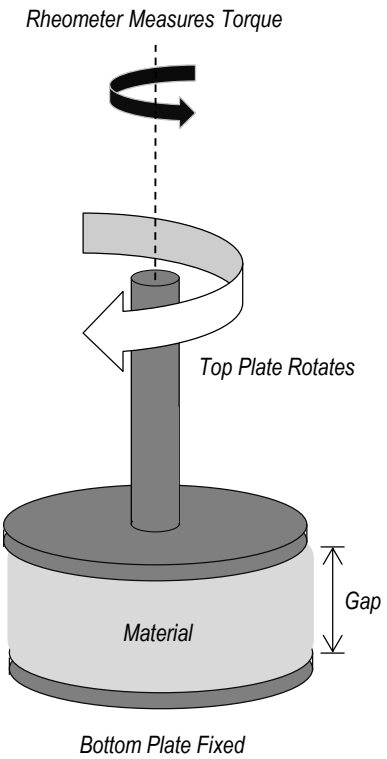

Figure 2-3. Parallel plate rheometer geometry.

Before testing begins, the top plate is raised above the bottom plate, which is fixed. A sample of material is loaded onto the bottom plate, and the top plate is lowered to within several millimeters of the bottom plate. The material being tested fully contacts both plates. The top plate then rotates at a given angular velocity, and a sensor in the rheometer measures the resulting torque. The viscosity of the material is calculated from the angular velocity and torque data. Varying the angular velocity allows the rheometer to measure the viscosity at different levels of applied shear.

2.6 Rheology Theory

The mechanical behavior of construction materials such as concrete and steel are dependent on their stress-strain properties. A simple stress-strain curve for steel is indicated in Figure 2-4.

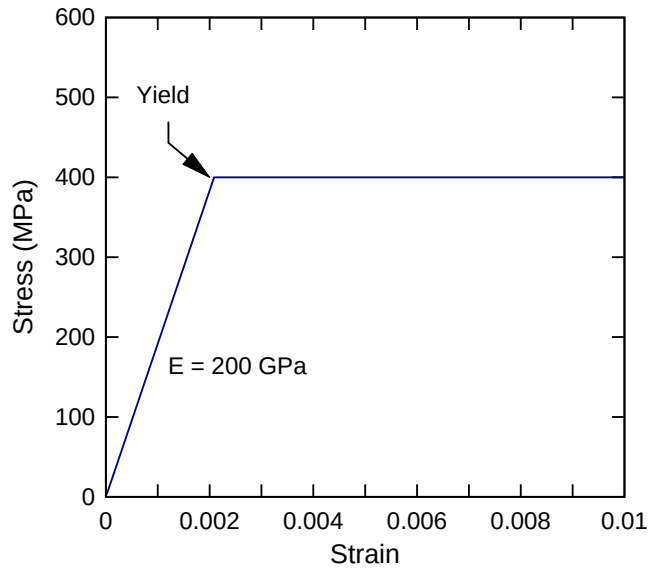

Figure 2-4. Simple stress-strain model for steel.

A dynamic shear rheometer (DSR) can be used to generate the equivalent of a stress-strain curve for a fluid material. The rheometer can impose shear on the materials at varying rates by applying different angular velocities. This action, called shear rate, can be thought of in the same manner as strain. The units of shear rate are s^{-1}. In general, a higher angular velocity corresponds to a higher shear rate. As it imposes varying shear rates, the rheometer measures torque which it converts to a shear stress. Shear stress can then be plotted against shear rate to generate the equivalent of a stress-strain curve for a fluid material. This curve is called a flow curve. (Hackley and Ferraris 2001)

In the same manner that the mechanical behavior of concrete and steel is based on the shape of their stress-strain curves, the mechanical behavior of a fluid material is

based on the shape of its flow curve. A flow curve for a Newtonian fluid is indicated in Figure 2-5.

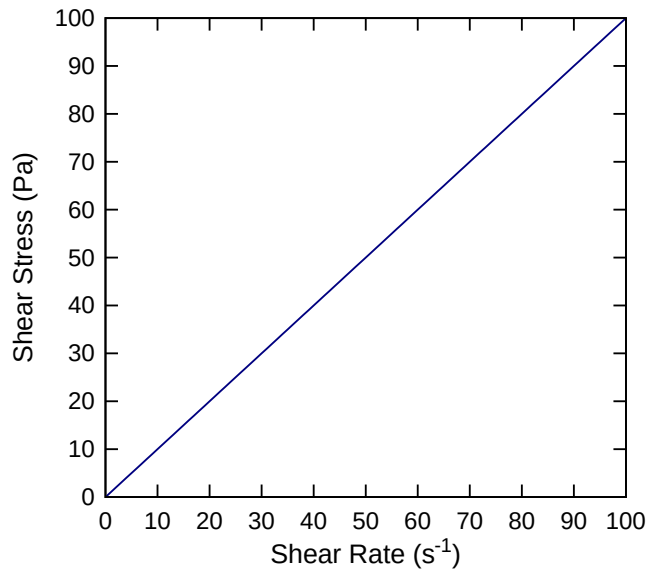

Figure 2-5. Flow curve for Newtonian fluid model.

A Newtonian fluid exhibits constant viscosity at any shear rate. Viscosity is the ratio of shear stress to shear rate (Hackley and Ferraris 2001); therefore the flow curve shown in Figure 2-5 represents a Newtonian fluid. Non-Newtonian flow curves take on different shapes, as shown in Figure 2-6.

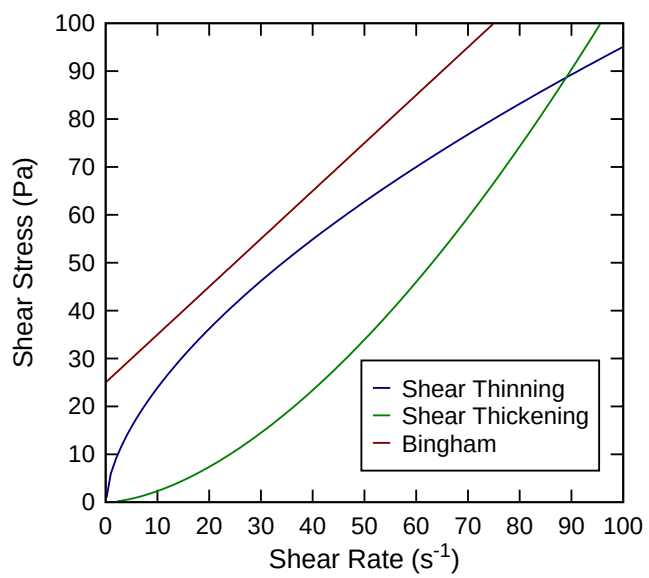

Figure 2-6. Flow curves for several non-Newtonian fluid models.

Depending on the shape of the flow curve, the non-Newtonian fluid can be classified in various manners. A shear-thinning fluid exhibits a decrease in viscosity with an increase in shear rate. (Hackley and Ferraris 2001) PT grout is an example of a shear-thinning fluid. The viscosity of a PT grout is meant to be very low during high shear applications, such as mixing and pumping, to reduce pumping pressures. However when the applied shear is reduced, as when the PT grout is sitting in the duct, the viscosity is meant to increase so that the grout doesn't flow out of position. Other non-Newtonian fluids are classified as shear-thickening, meaning that their viscosity increases as the applied shear rate increases. (Hackley and Ferraris 2001) An example of a shear-thickening fluid is cornstarch and water. The viscosity of cornstarch and water increases as the applied shear rate increases.

Another common material model for non-Newtonian fluids is the Bingham model. A Bingham fluid is essentially a Newtonian fluid that exhibits a yield stress. Below its yield stress, the material behaves in an elastic manner similar to concrete or steel before it has yielded. Above its yield stress, the material deforms and flows, behaving as a plastic. Materials that exhibit this property are also called viscoplastic. The viscosity of a Bingham material in its plastic state is constant with respect to shear rate. (Hackley and Ferraris 2001) The toothpaste from the earlier example is a Bingham fluid. It does not flow out of the tube until enough shear is applied to cause it to yield and flow. Some fluids that exhibit a yield stress are also shear-thinning or shear-thickening. In addition to having an elastic region, these fluids exhibit variable viscosity over a range of shear rates.

Time is another important variable to consider in the study of non-Newtonian fluids. Thixotropy is the model used to describe a material that exhibits time dependent rheological properties. Thixotropy is illustrated in Figure 2-7.

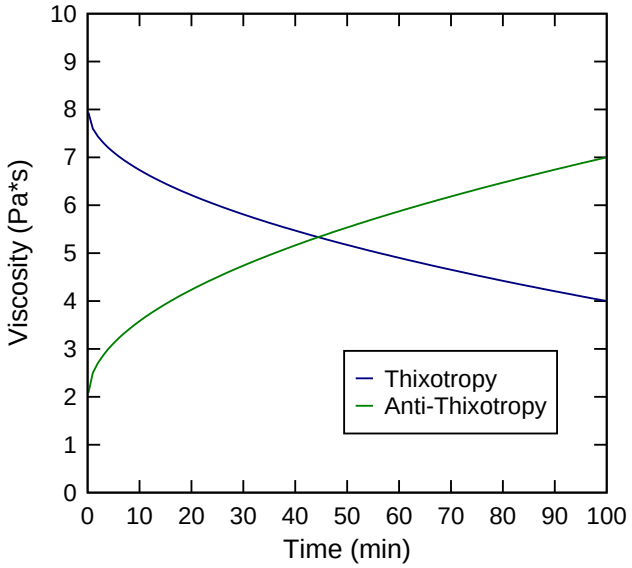

Figure 2-7. Thixotropic effects observed in material subjected to constant shear rate over a period of time.

A thixotropic material's viscosity will decrease over time where a constant shear rate is applied. An anti-thixotropic material's viscosity will increase over time where a constant shear rate is applied. (Hackley and Ferraris 2001) Both of these properties are reversible. Thixotropy occurs in many fluids, however it usually occurs in conjunction with shear-thinning or shear-thickening effects.

The Post-Tensioning Institute (PTI) specification (2012) defines thixotropy as "The property of a material that enables it to stiffen in a short time while at rest, but to acquire a lower viscosity when mechanically agitated, the process being reversible." This is not in agreement with the rheological definition presented in Chapter 2. The prepackaged grouts tested in this research stiffen quickly at rest, which is due to anti-

thixotropy. Furthermore, the decrease in viscosity when mechanically agitated is due to shear-thinning rather than thixotropy.

From a rheological standpoint, the mechanical behavior of different fluids is dependent on the shape of their flow curves. In addition to the flow curve, most materials display time-dependent thixotropic properties. PT grouts, which are proprietary mixtures of cement and other admixtures, can exhibit very different flow curves and thixotropic properties when compared to one another. Care must be taken to develop a test that allows the rheological properties of materials with unknown constituents to be compared.

2.7 DSR Testing of Grout

Four prevailing test methods for DSR testing of grouts and cement paste were given in the literature. These were the flow curve test, the stress growth test, the low-frequency oscillatory test, and the apparent viscosity test.

The most common test in the literature, the flow curve test, is run by testing the material over a range of shear rates. The shear stress is recorded and plotted against shear rate. This curve is called a flow curve, and various models can be fitted to the curve. The most commonly used model for grouts is the Bingham model, which provides values for yield stress and plastic viscosity. Ferraris & Gaidis (1992) studied the connection between the workability of concrete and the rheology of cement paste. Testing was conducted using a parallel plate rheometer. They used the flow curve test and applied the Bingham model. Khayat et al. (1999) made use of the Bingham model to determine the yield stress of grouts with high-range water-reducing admixtures. Yahia & Khayat (2003) performed a flow curve test on grouts containing various SCM. They showed that the Bingham model was not a good fit for grouts containing SCM. They

fitted various empirical models to the grouts containing various SCM to determine which model was most valid. Ultimately, they proposed a new model for use to characterize these grouts. Rosquoet et al. (2003) studied the rheology of fresh cement paste at high shear rates. They ran a flow curve test with higher shear rates than Ferraris & Gaidis (1992). They found that, when considering the higher shear rates, the cement paste behaved as a shear-thinning material. Amziane & Ferraris (2007) completed a study of the rheological properties of cement paste as it set using the Bingham model. Their research made use of a set of parallel plates, and showed that the Bingham model was not entirely appropriate for cement paste. The yield stress of the grouts could be determined, but the plastic viscosity could not. Petit et al. (2010) used the flow curve test to characterize the rheological properties of the grouts at high temperatures. They found that, as temperature increased, the yield stress of the grouts also increased.

The stress growth test is run by shearing the material at a very low shear rate over a period of several minutes. The shear stress is recorded and plotted vs. time. The yield stress point can be extracted from the shear stress versus time curve. Amziane & Ferraris (2007) ran several stress growth tests on cement pastes using a set of parallel plates. Their research showed that the stress growth test could be used to determine the yield stress of the cement pastes. Sant et al. (2008) used the stress growth test to evaluate the rheological properties of fresh grout. In addition, Dehadrai et al. (2009) made use of the stress growth test to attempt to locate the fluid-solid transition point of a cement paste. Their research showed that they could not determine this point using the stress growth test.

The literature also made mention of a low-frequency oscillatory test. In this test, the rheometer imposes very small oscillations on the material. The material does not

yield at these low frequencies, so this test provides insight into the elastic behavior of the material. The response of the material is measured, and a modulus can be plotted to determine the increase in stiffness of the material. Schultz & Struble (1993) studied the behavior of fresh cement paste using low amplitude oscillatory tests with a cup and bob geometry. They found that this was a valid way of studying the change in the elastic properties of a cement paste over time. Struble & Lei (1995) used creep/recovery tests to study the setting of cement paste with a cup and bob geometry. They determined that this was also a valid method of assessing the rheological properties of cement paste. Chen et al. (2006) completed additional research using the oscillatory tests to measure cement-admixture interaction. Al Martini & Nehdi (2009) studied the effects of high-range water-reducing admixtures and temperature on the rheology of grout. They made use of oscillatory sweep tests in their study. They observed higher stiffness values when the temperature of the grouts was increased, and lower stiffness values when the amount of high-range water-reducing admixtures was increased.

The apparent viscosity test received the least discussion of the four methods in the literature. The apparent viscosity is the viscosity of a material at a nominal shear rate. No explicit test method was provided in the literature, however several mentions of apparent viscosity were made. Khayat & Yahia (1998) ran a series of simultaneous flow cone and apparent viscosity tests on different grotus. Khayat et al. (1999) studied the rheology of grouts with high-range water reducing admixtures using a rheometer. These grouts were meant to mimic PT grouts. Their experimental setup made use of a cup and bob geometry. They ran a series of tests in which they determined the apparent viscosity at different shear rates. Amziane & Ferraris (2007) determined that the

apparent viscosity over a range of shear rates could be used to assess the flow capability of the grouts. They used a parallel plate geometry for testing.

2.8 DSR Geometry

Many geometries are available for DSR testing including parallel plates, cone and plate, and concentric cylinder geometries. Due to the constant thickness of the material between the plates and the uniform flow imposed by the rotation, formulas for the theoretical shear rate and shear stress are easily derived. More complex geometries, such as the cup and helical ribbon, and cup and vane geometries impose very complex movement on the material. Consequently, shear stress and shear rate are based on empirical calibrations using reference materials.

The serrated parallel plate geometry is the same as the parallel plate geometry, except that both of the plates have serrations. The serrated plates allow for the testing of suspensions with large particle sizes. Ferraris et al. (2007) showed that suspensions with large particles could not be tested using a standard set of parallel plates, because the particles in the suspension would jam. They showed that the serrated parallel plates could be used to test suspensions with large particle sizes, such as a mortar with sand.

The cup and vane geometry makes use of a vane inside of a cup for rheological measurements. The cup and vane is primarily used for yield stress testing with many different types of materials (Cullen 2003). The vane is assumed to act as a solid cylinder when it rotates inside the cup. Zhu et al. (2010) completed a numerical simulation to study the behavior of particles within a suspension as they were agitated by the vane. Their model showed that this assumption is incorrect.

The cup and helical ribbon geometry is more complex than the traditional geometries. It is not possible to calculate the shear rate and shear stress measured by

this rheometer given its complex shape. It offers several benefits, however. Suspensions with large particle sizes that cannot be tested using traditional geometries can be tested in the cup and ribbon. It also continuously mixes the material as it tests, which prevents larger particles from settling out. Ait-Kadi et al. (2002) demonstrated both of these properties by testing ketchup, which is a suspension with large particles that tend to flocculate. They were able to obtain repeatable flow curves when using the helical ribbon geometry; they were not able to do so with simple geometries. Cullen et al. (2003) explain that the helical ribbon can be used to determine how a suspension builds structure where other geometries cannot. The oscillatory test is used to do this. They also state that the helical ribbon has been used to study flow curves and apparent viscosity of suspensions in the past.

2.9 Relationship between Flow Cone and Rheology

Extensive research has been performed to determine whether or not different pieces of field equipment are suitable tools for performing quality-control checks. This research is useful to this project because it studies the relationship between field equipment, such as the flow cone, and laboratory equipment, such as the DSR.

Khayat & Yahia (1998) showed that the flow cone test is an accurate predictor of the apparent viscosity measured using a DSR where a high shear rate in the range of 340 to 510 s^{-1} is used for flow times in the range of 40 to 200 seconds. This shear rate range corresponds to the shear rates imposed on the grout during pumping and mixing operations in the field.

Le Roy & Roussel (2005) showed that the flow cone time is proportional to the Bingham plastic viscosity where the flow cone time is higher than 15 seconds and the material does not exhibit a high Bingham yield stress (above 20 Pa). These conclusions

were made using a concentric-cylinder DSR geometry. At a low viscosity, the relationship between flow cone time and Bingham plastic viscosity becomes non-linear.

Nguyen et al. (2006, 2011) have performed extensive research relating the marsh flow cone time to rheological properties if considering the tested fluid using the Herschel-Bulkley model. This research was conducted using a concentric cylinder DSR geometry. They developed a semi-analytical solution that allows for prediction of Herschel-Bulkley parameters given a flow cone time for cement grouts (Nguyen et al. 2006). This model was accurate for grouts that diverged from the Herschel-Bulkley model at very low shear rates due to HRWRA and VMA; PT grouts fall into this category. (Nguyen et al. 2011)

2.10 Shear Rates Imposed by Field Equipment

During the HTGF test the grout is subjected to a wide range of shear rates from the mixer, pump, and flow cone. In the field the grout is subjected to an additional low shear rate after it is placed in the duct. Khayat and Yahia (1998) state that shear rates of 340 to 510 s^{-1} occur in the field during mixing and pumping, based on results measured using a flow cone and DSR. They also state that grout experiences a shear rate of less than 5 s^{-1} after placement. Ferraris and Gaidis (1992) state that cement paste will experience a shear rate of 1 to 20 s^{-1} after placement

.

CHAPTER 3
APPROACH

The primary purpose of the HTGF test was to ensure that qualified grouts would not thicken excessively during pumping in hot-weather conditions. This research project was aimed at developing a test method that provided a more direct measure of the rheological properties of grout at high temperatures and did so with a test method more amenable to a typical construction materials testing laboratory's equipment. To develop an adequate replacement for the HTGF test, two aspects of the test were considered. The first was the measure of the fluidity of the grout, which the HTGF test handled using the flow cone. The second aspect was the conditioning of the grout in between sampling. The HTGF test imposed a dynamic mechanical shearing action on the grout in between sampling; this conditioning needed to be replicated to produce the same rheological response in the grout.

After settling on a geometry for testing, currently available DSR test methods were reviewed to determine if a suitable test was available. None of the currently available tests were found to be adequate to assess the rheological properties of the PT grouts. Due to the complex rheological properties of the commercially available PT grouts, the apparent viscosity test was developed so that all of the different grouts could be compared. The apparent viscosity test was run in conjunction with the HTGF test on four commercial PT grouts. Once the effects of the HTGF test's conditioning process on the rheological properties of the grout were known, two techniques were investigated to simulate the conditioning. Ultimately, several options are presented for the replacement of the HTGF test. The grout conditioning can be performed using either a laboratory-sized high shear mixer or the DSR. The fluidity assessment can be performed using

either a flow cone or the DSR. The flow chart shown in Figure 3-1 provides a summary of the research approach.

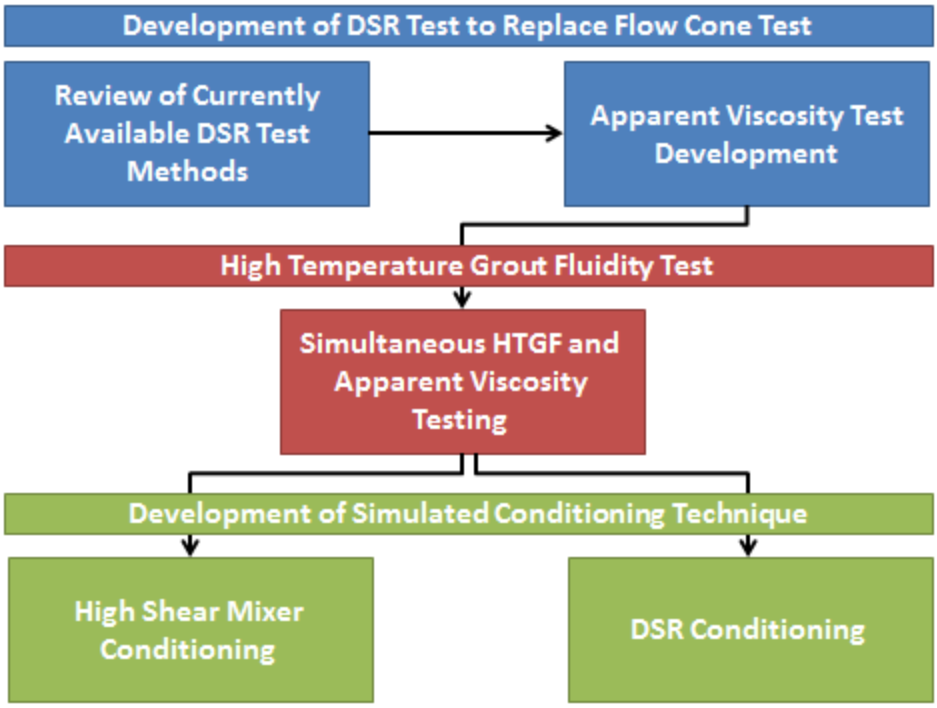

Figure 3-1. Flow chart depicting research approach.

CHAPTER 4
MATERIALS

Testing was conducted on both plain portland cement grouts and prepackaged PT grouts currently on the FDOT QPL. Plain grouts were investigated under a range of water-cement (w/c) ratios ranging from 0.40 to 0.45. Each of the commercial PT grouts were pre-packaged in a 50-lb or 55-lb bag. This bag contains the cement along with the various admixtures that give the PT grouts their specific properties. The manufacturers specify a certain amount of water that is meant to be mixed with one bag of grout. All PT grout samples were mixed over the entire range of the manufacturer's water content specifications.

Plain grouts were designed with codes such as C40 or C45. The "C" in the code indicates that the grout was a plain grout. The "40" or "45" indicates the water-to-cement ratio (i.e. 0.40 or 0.45). PT grouts were designated with codes PT1, PT2, PT3, and PT4. Each of the PT grouts received an additional number in their code (i.e. PT1-1 or PT3-2) to distinguish between different lots of the same material.

It is unlikely that the admixtures and cement are distributed homogenously throughout the pre-packaged bags of PT grout. When a partial bag of PT grout is sampled, it is likely that the sample will contain a higher percentage of either cement or admixtures than is found in the entire bag. Thus, a partial bag sample of PT grout is not representative of the material that the manufacturer has produced. For this reason, full bags of PT grouts were mixed. Partial bags should not be sampled and mixed.

CHAPTER 5
MIXING AND AGITATION EQUIPMENT

Three different mixers were studied during the course of research: a colloidal grout plant, a high shear sanitary mixer, and a blender mixer. Each of these mixers imposed a high shear rate to fully mix the grout samples. It is difficult to quantify the exact shear rate imposed by each mixer. The primary difference between the three mixers is the volume of grout that each can mix. Table 5-1 contains a summary of the volumes that each mixer is capable of mixing. One 50-lb bag of prepackaged PT grout yields about 0.5 cubic feet of grout when mixed with water.

Table 5-1. Comparison of mixing volume for each mixer.

Mixer	Mixing Volume
Colloidal grout plant	2 – 10 c.f.
High shear sanitary mixer	0.25 – 0.75 c.f.
Blender mixer	0.015 – 0.035 c.f.

5.1 Colloidal Grout Plant

Typically, a colloidal grout plant is used to mix and pump large quantities of grout in the field. It is unusual to find a colloidal grout plant in a construction materials testing laboratory because it is a large, production-oriented piece of equipment. The mix tank and agitation tank on a typical colloidal mixer are shown in Figure 5-1. The pump, which is not visible in the photograph, is located below the platform on the mixer. The colloidal mixer was equipped with a centrifugal diffuser-type pump rotating at speeds up to 2,000 RPM that disperses the cementitious material down to its finest particle size to achieve complete particle wetness. The agitator tank is equipped with a variable speed high-efficiency paddle mixer that prevents the grout from building structure before it is pumped. The grout pump, which is connected directly to the agitator tank, is a size six, three stage progressing cavity, positive displacement, rotor-stator pump. (ChemGrout)

Figure 5-1. Chemgrout CG600 13 c.f. colloidal grout plant with various parts labeled. Photo courtesy of Alex Piper.

The mixer was powered by a 375-cfm diesel air compressor (Figure 5-2)

Figure 5-2. 375-cfm diesel air compressor used to power grout plant. Photo courtesy of Trey Hamilton.

The following procedure was used to mix and pump grout in the colloidal grout plant:

1. Add water to mix tank and turn on colloidal mixer and agitator paddle. See Figure 5-3.

2. Add one bag of grout at a time. Add grout over a period of 20-30 seconds per bag. See Figure 5-4.

3. Continue running colloidal mixer and agitator paddle for 2 minutes after adding last bag of grout. See Figure 5-5.

4. Transfer the grout to the agitation tank and start the paddle in the agitation tank.

5. Pump grout to target. See Figure 5-6.

Figure 5-3. Add water to mix tank. Photo courtesy of Trey Hamilton.

Figure 5-4. Add one bag of grout at a time. Photo courtesy of Trey Hamilton.

Figure 5-5. Continue running colloidal mixer and agitator paddle for 2 minutes after adding last bag of grout. Photo courtesy of Trey Hamilton.

Figure 5-6. Pump grout to target. Photo courtesy of Trey Hamilton.

5.2 High Shear Mixer

In addition to the colloidal mixer, a high shear sanitary mixer was also investigated (Figure 5-7). The high shear mixer was well-suited to mix one 50-lb bag of PT grout at a time. The high shear mixer contained both a low speed impeller and high speed impeller, which could be operated independently. The low speed anchor style impeller could operate at speeds up to 35 RPM. The high-speed saw-blade style impeller could operate at speeds up to 3,500 RPM. The mix tank was jacketed by a hollow-wall, which when combined with a water bath allowed for precise temperature control during mixing. The mix tank also contained an air-actuated valve for sampling.

(a) (b)

Figure 5-7. High shear mixer used to prepare grout samples (a) and impellers (b). Photo courtesy of Alex Piper.

The following procedure was used to mix grout in the high shear mixer:

1. Set the water bath to desired testing temperature.

2. Pour the water into the mix tank and run the low speed impeller at 35 RPM until the water is heated to the testing temperature. See Figure 5-8.

3. Continue to run the low speed impeller at 35 RPM. Turn the high speed impeller on to 3,500 RPM.

4. Add the dry material over a period of 3-5 minutes. Add slowly enough to avoid clumping of dry material. See Figure 5-9.

5. Once all dry material has been added, continue to run both impellers for 30 seconds.

6. Turn the impellers off, raise the mixer head, and scrape the mixer blades and walls of the mixer bowl over a period of 2 minutes. See Figure 5-10.

7. Lower the mixer head back into the mix tank. Run the low speed and high speed impellers at 35 and 3,500 RPM respectively for 90 seconds.

Figure 5-8. Pour water into the mix tank. Photo courtesy of Trey Hamilton.

Figure 5-9. Add dry material to mixer over a period of 3-5 minutes Photo courtesy of Trey Hamilton.

Figure 5-10. Raise mixer head and scrape low speed agitator paddle. Photo courtesy of Trey Hamilton.

5.3 Blender Mixer

The blender mixer was used to perform small-scale mixing. The blender was placed in series with a timer and speed controller that allowed for a repeatable mixing procedure. The mixer could be operated at an angular velocity range from 500 RPM to 20,000 RPM. Figure 5-11 shows the blender on the right and the timer and speed controller on the left. Figure 5-12 shows the blade configuration in the blender. The wide blades allowed the mixer to impose a high shear rate on the grout, which caused the cement particles to disperse completely into the water. In addition, the blender was connected to a temperature-controlled water bath. This allowed control over the mixing temperature.

Figure 5-11. Waring HGBTAC30 commercial blender used for mixing. Photo courtesy of Alex Piper.

Figure 5-12. Blade configuration used in mix procedure with quarter shown for reference. Photo courtesy of Alex Piper.

The following procedure, which was based on ASTM C1738 (2011), was used to mix grout in the blender mixer:

1. Set the temperature controller to desired testing temperature.
2. Pour the water into the mixer and agitate at 4,000 RPM for 15 seconds.
3. While the mixer continues to run at 4,000 RPM, add the dry material over a period of 60 seconds.
4. Once all dry material has been added, run the mixer at 12,000 RPM for 30 seconds.
5. Turn the mixer off and allow the sample to rest for 2 minutes.
6. Run the mixer at 12,000 RPM for 90 seconds.

After mixing, the grout was stored in a pre-heated stainless steel Thermos container which maintained the temperature to within 3°F of the initial temperature over the duration of one hour. The grout was agitated using a plunger mixer (Figure 5-13) within 30 seconds of drawing a sample to test. This ensured that the sample was homogenous.

Figure 5-13. Plunger mixer used to agitate grout before testing. Photo courtesy of Alex Piper.

CHAPTER 6
DYNAMIC SHEAR RHEOMETER EQUIPMENT

The TA AR2000ex Dynamic Shear Rheometer (Figure 6-1) was used for test method development. The torque range on the rheometer was 0.0001 to 200 mN*m. The torque range needed for test method development was approximately 0.5 to 20 mN*m. The maximum angular velocity was 300 rad/sec. For test method development, the maximum angular velocity was approximately 70 rad/sec.

The DSR was controlled by a computer program which input angular velocity parameters to the DSR and recorded torque measurements. The software automatically calculated shear rate, shear stress, and viscosity from the angular velocity and torque data. The software also allowed for control of sample temperature during testing.

Figure 6-1. TA AR2000ex Dynamic Shear Rheometer with helical ribbon and cup geometry. Photo courtesy of Alex Piper.

6.1 DSR Geometries

Two different stainless steel geometries were used with this rheometer: stainless steel serrated parallel plates and stainless steel cup and helical ribbon.

6.1.1 Serrated Parallel Plates

A set of stainless steel serrated parallel plates were considered as a part of the DSR test method development. The serrated parallel plates were 40 mm in diameter. The hatches were formed at an angle of 90° relative to the plate and were 0.5mm deep. A photograph of the plates is shown in Figure 6-2.

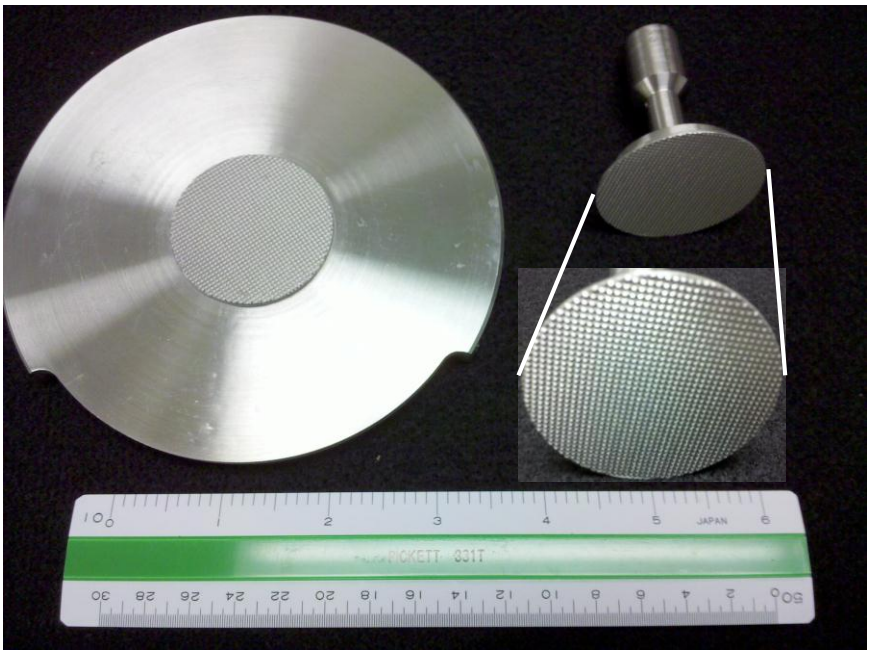

Figure 6-2. Serrated parallel plate DSR geometry – bottom plate (left) and top plate (right). Photo courtesy of Alex Piper.

The serrations on the parallel plate allow for testing of suspensions with large particle sizes, as shown by Ferraris et al. (2007). If flat plates are used for testing suspensions with large particles, the particles can jam together and invalidate the test. Some of the PT grouts contain large particle sizes, so the serrations provide an advantage over the traditional parallel plates.

Equation 6-1 and Equation 6-2 show how shear rate and shear stress were calculated using the parallel plates. If the serrated parallel plate geometry is used, a correction factor must be applied (Ferraris et al. 2007). The formula for correcting the viscosity of the plates is given in Equation 6-3.

$$\dot{\gamma} = \frac{\omega * r}{h} \tag{6-1}$$

where $\dot{\gamma}$ is the shear rate, ω is the angular velocity, *r* is the radius of the plate, and *h* is the distance between the plates.

$$\tau = T * \frac{1}{\frac{2}{3} * \pi * r^3} \tag{6-2}$$

where τ is the shear stress, *T* is the torque measured by the rheometer, and *r* is the radius of the plate.

$$\eta_c = \eta * (1 + \frac{c}{h}) \tag{6-3}$$

where η_c is the corrected viscosity (mPa*s), η is the viscosity measured using the serrated plate (mPa*s), c is the gap correction value (0.32 mm for the set of plates that were investigated), and h is the size of the gap (mm).

6.1.2 Cup and Ribbon

In addition to the serrated parallel plates, a stainless steel cup and helical ribbon geometry was investigated. A photograph of the cup and ribbon geometry is shown in Figure 6-3. The dimensions of the cup and ribbon geometry are given in Figure 6-4.

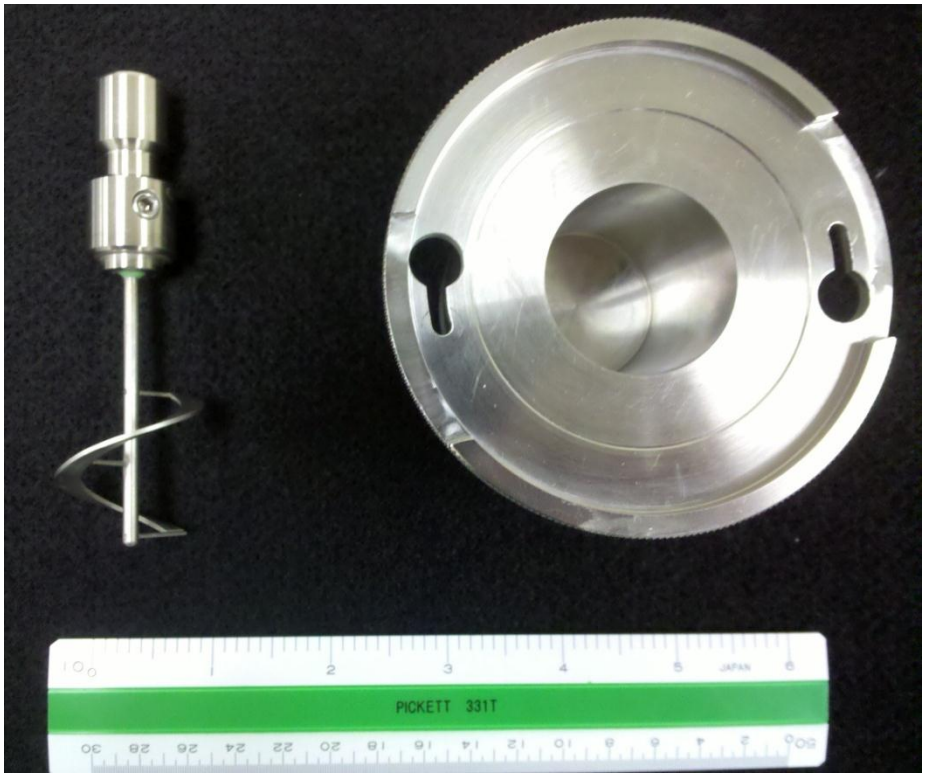

Figure 6-3. Helical ribbon (left) and cup (right) DSR geometry. Photo courtesy of Alex Piper.

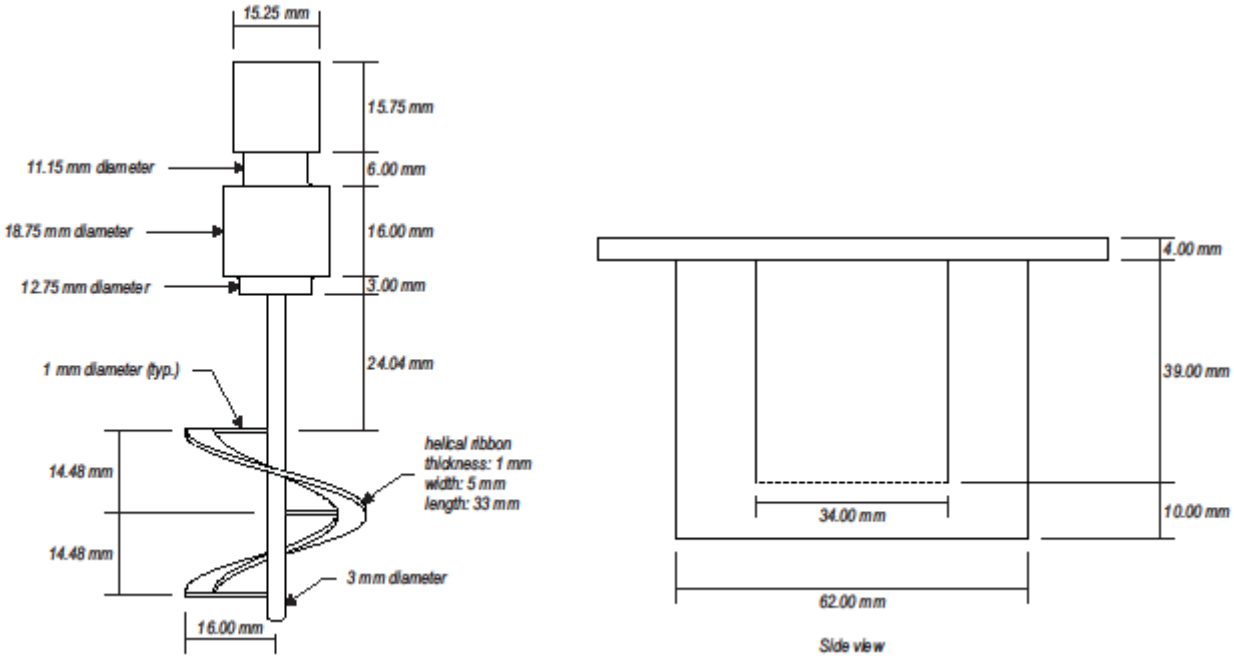

(a) (b)

Figure 6-4. Dimensions of helical ribbon (a) and cup (b) DSR geometry.

The cup and ribbon geometry was used because it would prevent sedimentation over long test periods. The cup and ribbon geometry allowed for the testing of a suspension with larger particle sizes than the serrated parallel plate may allow. The cup and ribbon also allowed for the testing of materials with a very low viscosity, which may flow off of the parallel plates during testing. The cup is enclosed by a Peltier Jacket (not shown), which precisely controls sample temperature during testing. The equipment is used for testing by filling the cup with grout, and then lowering the ribbon into the cup. The ribbon rotates at a given angular velocity, and the DSR measures the corresponding torque.

The helical ribbon was empirically mapped to the parallel plate geometry by the manufacturer using the Couette Analogy. This was accomplished by determining average stress coefficients for the helical ribbon and using these to calculate stress from the strain measured by the rheometer (Franck). The manufacturer of the rheometer provided a coefficient for the shear rate based on the shape of the geometry. Equation 6-4 and Equation 6-5 show how shear rate and shear stress are calculated using the helical ribbon geometry.

$$\dot{\gamma} = F_{\dot{\gamma}} * \omega \tag{6-4}$$

where $\dot{\gamma}$ is the shear rate, $F_{\dot{\gamma}}$ is the shear rate factor, and ω is the angular velocity. $F_{\dot{\gamma}}$ is equal to 2.460 for the helical ribbon geometry.

$$\tau = F_{\sigma} * T \tag{6-5}$$

where τ is the shear stress, F_{σ} is the shear stress factor, and T is the torque measured by the rheometer. The values of F_{σ}, as given by the manufacturer was 2,730 m^{-3} for the helical ribbon geometry. The value of F_{σ} was later determined to be 20,480 m^{-3} after calibrating the rheometer using a NIST standard reference material.

6.2 Cup and Ribbon Geometry Calibration

To use the cup and ribbon geometry for testing of PT grouts, it was necessary to ensure that the results were repeatable across multiple laboratories. During preliminary

investigations on the grouts, the stresses measured using the cup and ribbon geometry did not match those measured using the parallel plate geometry when using the shear stress factor provided by the manufacturer.

Several standard materials were considered to calibrate the cup and ribbon geometry. A standard oil was inadequate for calibration. The oil was not a suspension and did not exhibit a yield stress. PT grouts exhibit both of these properties. Instead, a NIST standard material was used to determine a more appropriate shear stress factor. The NIST material was a suspension that exhibited a yield stress. The NIST standard material is available to the general public for purchase, allowing anyone to calibrate a cup-and-ribbon type rheometer in the future.

6.2.1 Reference Material

The NIST Standard Reference Material (SRM) 2492, “Bingham Paste Mixture for Rheological Measurements”, was used to calibrate the shear stress measured using the cup and ribbon geometry to the shear stress measured using a standard parallel plate geometry. The material was a mixture of corn syrup and limestone. The SRM included instructions for sample preparation and testing.

The reference material was a suspension that behaved as a Bingham plastic. A Bingham plastic is a viscoplastic material that exhibits a yield stress. If the material is below its yield stress, it behaves as a solid. If the yield stress is exceeded, the material deforms and flows. A typical flow curve for a Bingham plastic is indicated in Figure 6-5.

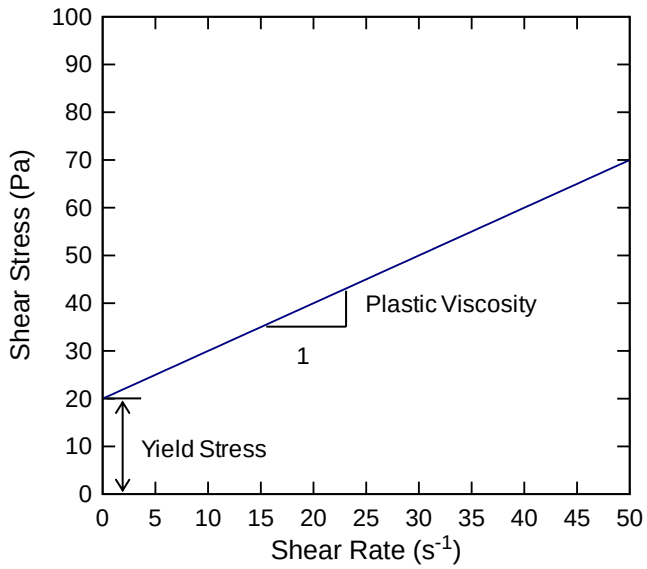

Figure 6-5. Flow curve for Bingham plastic material.

A Bingham plastic should exhibit linear flow curve behavior. The yield stress is the y-intercept on the stress-strain curve while the plastic viscosity is the slope of the curve. The material typically yields at a very low stress, which can be difficult to measure using a DSR. For this reason, the yield stress is generally extrapolated from the other data.

The SRM had a certified yield stress (Figure 6-6) and plastic viscosity (Figure 6-7) over a period of seven days after mixing. In addition to an expected mean value, standard uncertainty and expanded uncertainty values were provided. The standard uncertainty limits represent the standard deviation of the values measured during NIST testing. The expanded uncertainty limits represent a 95% confidence level.

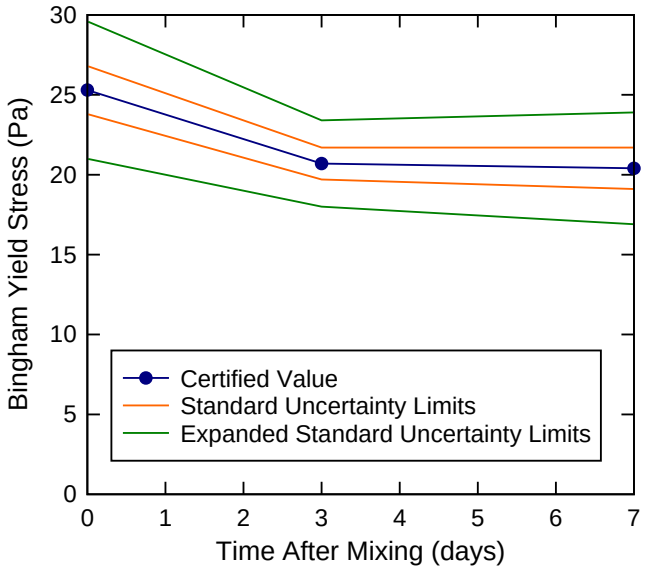

Figure 6-6. NIST certified Bingham yield stress values with respect to time after mixing.

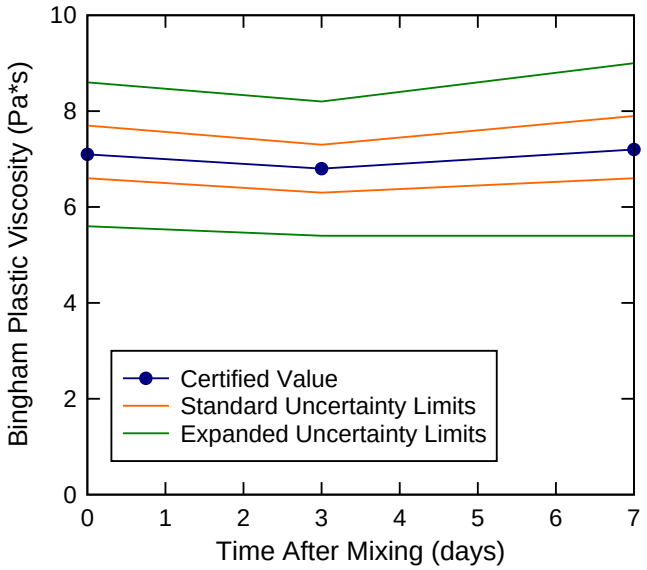

Figure 6-7. NIST certified Bingham plastic viscosity values with respect to time after mixing.

6.2.2 DSR Calibration Results

The SRM was tested using the DSR with the cup and ribbon geometry to determine appropriate shear stress calibration factors.The following test procedure was used to generate a flow curve:

1. Prepare sample according to ASTM C1738 (2011).

2. Load the material into the cup and ribbon geometry.

3. Shear the material at a rate of 0.01 s^{-1} for a period of 150 seconds.

4. Shear the material at a rate of 0.1 s^{-1}. Sample every 1 second. If 3 consecutive points are within 5% of each other, the material has reached equilibrium. Record the equilibrium stress value.

5. Repeat step 4 over the following shear rates: increase from 0.1 s^{-1} to 50 s^{-1} over 10 discrete points. Decrease from 50 s^{-1} to 0.1 s^{-1} over 20 discrete points. Record equilibrium stress for each point.

6. Plot shear stress vs. shear rate and determine appropriate Bingham parameters.

Two batches of SRM were prepared and tested. The first batch was not prepared with distilled water, as specified in the certificate. The second batch was prepared with distilled water. Results of the flow curve test for the SRM prepared with tap water on the same day as mixing are indicated in Figure 6-8.

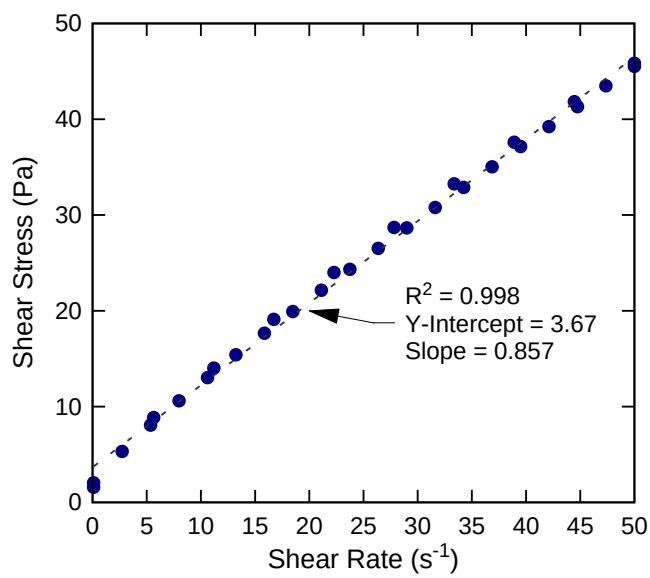

Figure 6-8. Flow curve results for SRM on the same day as mixing.

If a linear trend line is fitted to the flow curve in Figure 6-8, the yield stress was 3.67 Pa while the plastic viscosity was 0.857 Pa*s. The R^2 value was 0.998.

The flow curve test was run on the material on the following times after mixing: 0 days, 3 days, and 7 days. A plot of the ratio of the certified Bingham yield stress to that

measured using the cup and ribbon geometry for the batch prepared with tap water is provided in Figure 6-9. A similar plot for the batch prepared with distilled water is provided in Figure 6-10.

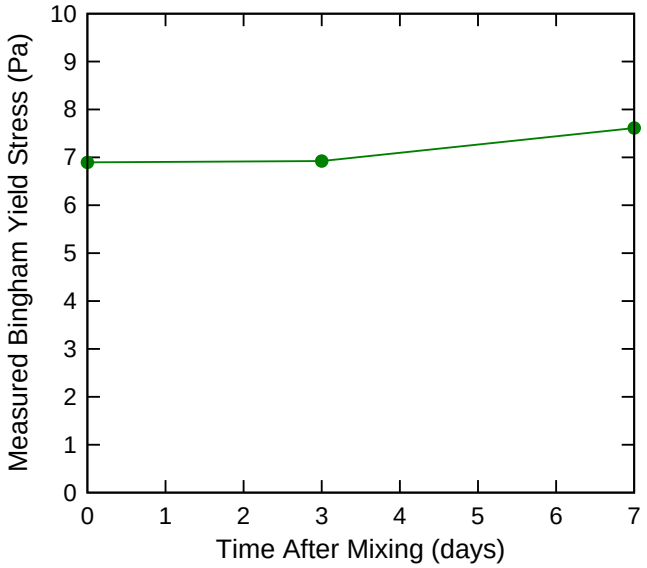

Figure 6-9. Ratio of certified Bingham yield stress to measured Bingham yield stress with respect to time after mixing for batch prepared with tap water.

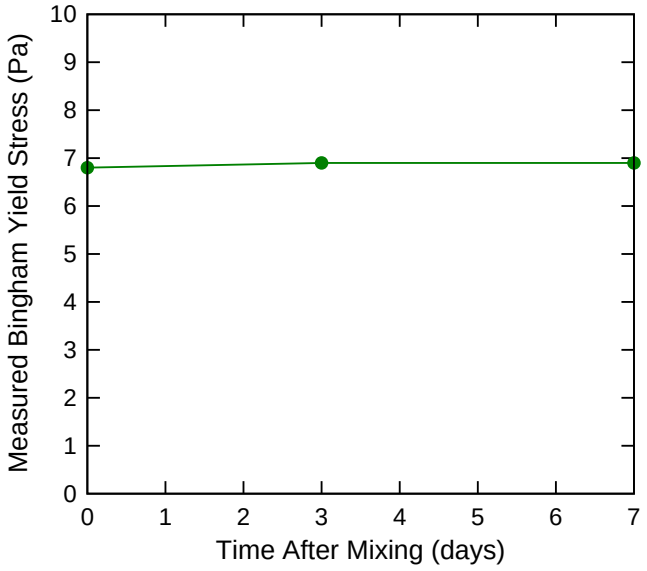

Figure 6-10. Ratio of certified Bingham yield stress to measured Bingham yield stress with respect to time after mixing for batch prepared with distilled water.

A plot of the ratio of the certified Bingham plastic viscosity to that measured using the cup and ribbon geometry for the batch prepared with tap water is provided in Figure 6-11. A similar plot for the batch prepared with distilled water is provided in Figure 6-12.

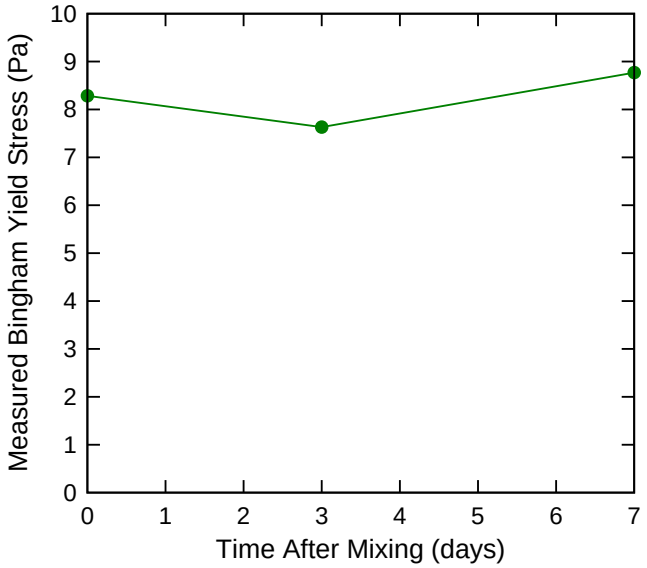

Figure 6-11. Ratio of certified Bingham plastic viscosity to measured Bingham yield stress with respect to time after mixing for batch prepared with tap water.

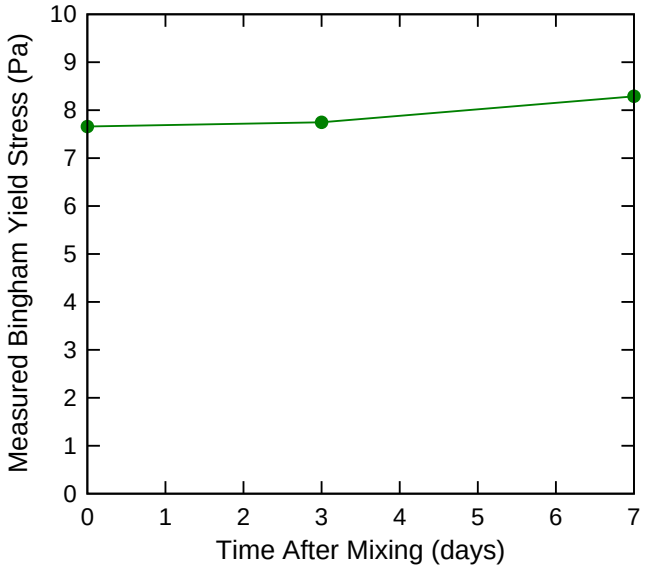

Figure 6-12. Ratio of certified Bingham plastic viscosity to measured Bingham yield stress with respect to time after mixing for batch prepared with distilled water.

Table 6-1 provides a summary of the measured Bingham values for both sets of tests as well as the ratios shown in the plots in Figure 6-9, Figure 6-10, Figure 6-11, and Figure 6-12.

Table 6-1. Summary of measured Bingham standard material values.

	Measured values					
	Yield stress (Pa)			Plastic viscosity (Pa*s)		
Water	Age (d)	Value	Ratio	Age (d)	Value	Ratio
	0	3.67	6.9	0	0.857	8.3
Tap water	3	2.99	6.9	3	0.891	7.6
	7	2.68	7.6	7	0.821	8.8
	0	3.74	6.8	0	0.927	7.7
Distilled water	3	3.02	6.9	3	0.878	7.7
	7	2.98	6.9	7	0.869	8.3

Equation 6-6 and Equation 6-7 were used to adjust the measured yield stress and plastic viscosity to the corresponding certified values.

$$\tau_A = A * \tau \tag{6-6}$$

where τ_A is the adjusted yield stress, A is the adjustment factor, and τ is the yield stress measured by the rheometer.

$$\eta_A = A * \eta \tag{6-7}$$

where η_A is the adjusted plastic viscosity, A is the adjustment factor, and η is the plastic viscosity measured by the rheometer.

The adjustment factor, *A*, is the same number in both Equation 6-6 and Equation 6-7. The adjustment factor was determined by averaging the twelve ratios of the Bingham parameters indicated in Table 6-1. Using this approach, an adjustment factor of 7.5 was determined. Figure 6-13 and Figure 6-14 contain plots showing the adjusted Bingham yield stress and adjusted Bingham plastic viscosity with respect to time after mixing respectively.

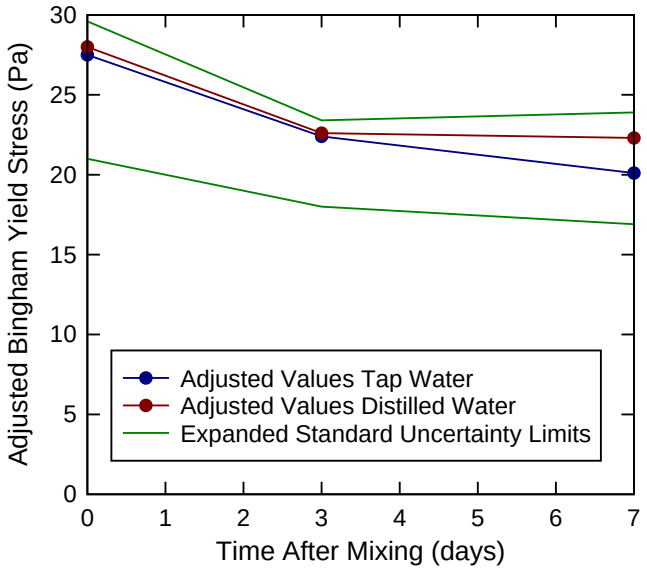

Figure 6-13. Variation in adjusted Bingham yield stress with respect to time after mixing.

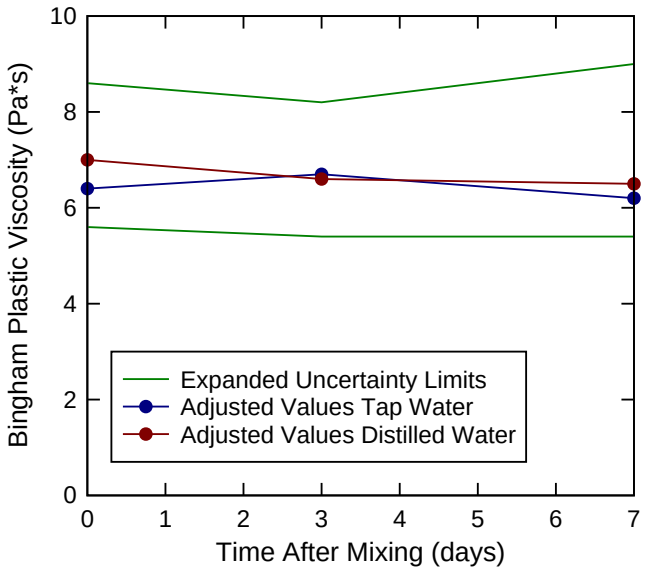

Figure 6-14. Variation in adjusted Bingham plastic viscosity with respect to time after mixing.

An adjustment factor of 7.5 provides good results. The adjusted yield stress and the adjusted plastic viscosity are both within the expanded uncertainty limits of the SRM for both batches. The adjustment factor was applied to the DSR by multiplying the manufacturer's shear stress factor by 7.5. The adjusted shear stress factor for the DSR, F_σ, was 20,480 m^{-3}.

6.3 DSR Geometry Selection

Two rheometer geometries were studied as a part of the DSR testing program: the serrated parallel plate geometry and the cup and ribbon geometry. It was necessary to decide on one geometry for the test procedure so that the results could be reproduced in other laboratories.

The primary advantage of the parallel plate geometry for the testing of cement paste is that the gap between the plates can be adjusted to simulate the spacing between aggregates in concrete (Ferraris and Gaidis 1992). This is done to predict the rheological properties of concrete based on the rheological properties of the cement paste. Because the PT grouts tested are not used as part of a concrete mixture, it is unnecessary to simulate aggregate spacing.

Both the serrated parallel plates and the helical ribbon allow for the testing of suspensions with large particle sizes. The size of the gaps between the serrated plates was dependent on the largest particle size in the suspension; the cup and ribbon had no such requirement. Because the PT grouts are all proprietary mixtures with different maximum particle sizes, a distinct gap parameter would be required to test each grout. This would complicate tests on future PT grouts that have not yet been developed, and increase the likelihood of error during testing.

The helical ribbon allows for testing over a longer time domain than the parallel plates. The primary advantage of the helical ribbon geometry is that it prevents particle settlement during testing. This allows longer test times, such as one hour, that may not be possible with the serrated parallel plates. Temperature control was another important factor for each geometry. The bottom plate in the parallel plate geometry was temperature controlled, but the top plate was not. Even when the top plate was left in

contact with the bottom plate for approximately 5 minutes prior to testing, the temperature of the top plate was about 8°F lower than the bottom plate when the bottom plate was 90°F. This results in the sample temperature dropping during testing over long periods of times. The cup, however, is enclosed by a Peltier jacket, which precisely maintains the sample temperature in the cup over long testing durations.

While running tests, some sample loading issues were noted with the parallel plates. The cement pastes, even at a relatively high w/c ratio such as 0.5, were much more viscous than the PT grouts. If using the parallel plates, the material must not flow over the edge of the bottom plate to satisfy the inherent no-slip assumption of the geometry. Because the PT grouts had a very low viscosity, some grout would flow out of the gap between the plates. Previous research performed on grouts with viscosity-reducing admixtures, such as that by Khayat et al. (1999), has also found that the cup-type rheometer geometry is more effective than parallel plate geometries for low viscosity grouts.

The primary disadvantage of the cup and ribbon geometry is that it does not allow for the exact calculation of shear stress and shear rate. However, by using the NIST SRM 2492 to calibrate the geometry, repeatable results can be obtained in multiple laboratories. Anyone using a cup and ribbon geometry can calibrate their rheometer using the SRM.

For these reasons, it was decided that the cup and ribbon geometry would be the most suitable for PT grout testing.

CHAPTER 7
REVIEW OF CURRENTLY AVAILABLE DSR TEST METHODS

The HTGF test made use of the flow cone to assess the fluidity of the grout every 15 minutes. To replace the HTGF test, it was necessary to use a DSR test method that allowed for comparison between plain and PT grouts. The literature showed that several currently available test methods were applicable to DSR testing of grout. These included the flow curve test, stress growth test, and oscillatory time sweep test. In addition to reviewing currently available test methods, an appropriate range of shear rates for testing was determined.

7.1 Testing Shear Rates

The literature indicated that a wide range of shear rates were used to assess the rheological properties of grouts. To determine an appropriate shear rate domain for PT grout testing, the shear rate imposed by a flow cone nozzle was calculated. The actual shear rate at the outlet of the flow cone nozzle is dependent upon the viscosity of the grout which is being discharged as well as the geometry of the nozzle. A closed-form solution for this does not exist; the calculation of shear rate in the flow cone nozzle for a non-Newtonian fluid is very complex. For this reason, it was assumed that the material in the nozzle was Newtonian. This should provide a good order-of-magnitude for the shear rates used in testing. The equation for calculation of the shear rate of a Newtonian fluid at the wall of a pipe is given in Equation 7-1.

$$\dot{\gamma} = \frac{4Q}{\pi r^3} \tag{7-1}$$

where $\dot{\gamma}$ is the shear rate, Q is the flow rate of the material in the pipe, and r is the radius of the pipe.

The flow cone efflux time of the grout has an impact on the shear rate calculation. Assuming a 30-second flow cone efflux time, which corresponds to the

failure limit, the flow rate of the grout in the nozzle is 2.03 in^3/sec. The shear rates imposed by different sized flow cone nozzles at this flow rate are given in Table 7-1.

Table 7-1. Summary of shear rates imposed by flow cone nozzle.

Shear rate	Flow cone nozzle diameter
165 s^{-1}	½ inch
50 s^{-1}	¾ inch

7.2 Flow Curve Test

The flow curve test was used extensively by previous researchers studying grout including Ferraris & Gaidis (1992), Khayat et al. (1999), Yahia & Khayat (2003), Rosquoet et al. (2003), Amziane & Ferraris (2007), and Petit et al. (2010).

The result of the flow curve test is a shear stress versus shear rate curve, called a flow curve. Various models can be fitted to the flow curve, the most common of which is the Bingham model, as discussed by Ferraris and Gaidis (1992). The procedure used for the flow curve test is as follows:

1. Mix grout according to the mix procedure in high shear mixer with water bath set to 90°F. The grout materials are stored at room temperature.
2. Load a sample of the grout into the DSR.
3. Pre-shear grout at 165 s^{-1} for 30 seconds. Sample every 1 second.
4. Allow grout to rest for 30 seconds.
5. Ramp shear rate from 0.1 s^{-1} to 165 s^{-1} continuously over a period of 3 minutes. Sample every 1 second.
6. Plot shear stress vs. shear rate. Fit model to data.

There was not much guidance in the literature as to the best range for the shear rate ramp. A maximum shear rate of 165 s^{-1} was selected because it was the shear rate calculated in the nozzle of the ½” flow cone. The test was conducted on all of the grouts several times over the period of one hour after mixing. Results of the test for grout C40 21 minutes after mixing are given in Figure 7-1.

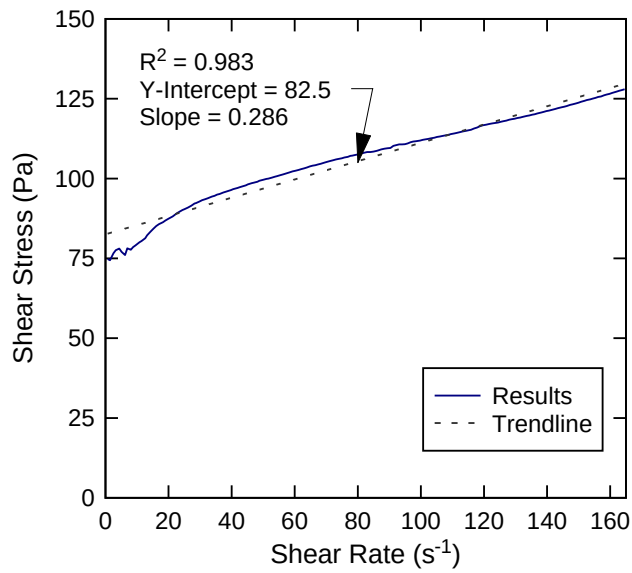

Figure 7-1. Flow curve for grout C40, 21 minutes after mixing.

To apply the Bingham model, the material must exhibit a linear flow curve, as shown in Figure 6-5. This curve exhibits a good linear trend, and the Bingham model can be applied with an R^2 value of 0.983. This results in a yield stress of 82.5 Pa and a plastic viscosity of 286 mPa*s. Additionally, the shear stress values measured here are similar to those measured by Amziane & Ferraris (2007).

Results of the flow curve test for grouts PT1-3, PT2-3, PT3-2, and PT4-3 mixed at the mid-range of the manufacturer's specified water content are given in Figure 7-2.

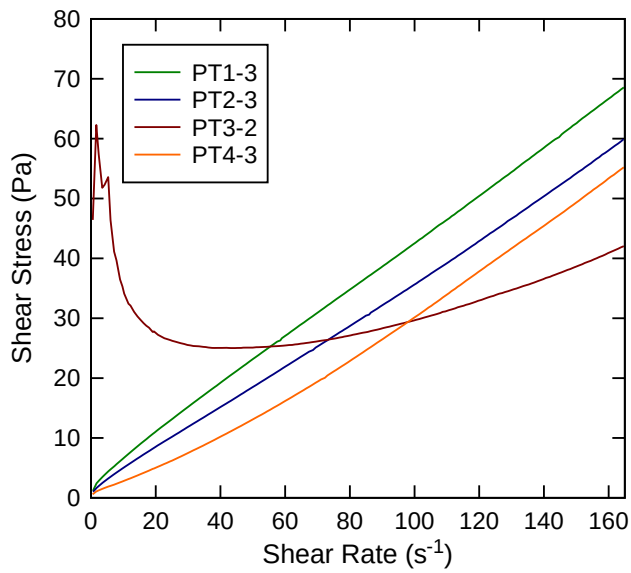

Figure 7-2. Flow curve for materials PT1-3, PT2-3, PT3-2, and PT4-3.

The Bingham model can be applied to the flow curves for grouts PT1-3 and PT2-3 because both exhibit a linear trend.

Grout PT4-3 also exhibits linear flow curve behavior, so it seems that the Bingham model can be applied. A linear fit results in an R^2 value of 0.994. However, the y-intercept of the trend line is negative, which would mean that the yield stress is negative. The Bingham model is not appropriate for grout PT4-3 because it predicts a nonsensical yield stress value.

Grout PT3-2 exhibits both shear-thinning and shear-thickening properties, which results in nonlinear flow curve behavior. The Bingham model cannot be applied to grout PT3-2 because of the non-linearity of the flow curve.

Previous research using the Bingham model was performed on plain grouts, to which it could successfully be applied to measure the yield stress (Amziane and Ferraris 2007). The results presented here agree that the Bingham model is applicable to plain grouts. However, the Bingham model cannot be used to assess the rheological

properties of the PT grouts. For grout PT4-3, it results in the measurement of a negative yield stress. For grout PT3-2, the flow curve was nonlinear.

There may be separate models that can be fit to the individual flow curves for each of the PT grouts. However, this would not allow for a comparison between the PT grouts. Further, even if all of the tested PT grouts could be described by a single model, future grouts may be developed that cannot be described by the same model. This would make it impossible to qualify certain new PT grouts in the future.

7.3 Stress Growth Test

Stress growth testing on cement pastes is reported in Amziane & Ferraris (2007). Both plain and PT grouts exhibit viscoplastic behavior, meaning that they should reach a certain yield stress for a given shear rate, marking the transition from solid-like behavior to fluid-like behavior. In the stress growth test, the yield stress of a grout is measured every 15-30 minutes to determine the change in yield stress with respect to time after mixing. In this test method, the grout must yield (i.e. begin to flow) to measure the yield stress. A very low shear rate is imposed on the grout so that a well-defined yield point can be captured. The procedure for measuring yield stress was as follows:

1. Set the Peltier Jacket temperature to 90°F.
2. Mix grout according to the mix procedure in high shear mixer or blender mixer. The grout materials are stored at room temperature.
3. Load a sample of the grout into the DSR.
4. Subject the grout to a shear rate of 0.1 s^{-1} for a period of 5 minutes.
5. Clean the grout out of the cup and, after 30 minutes, load a new sample of grout into the cup.
6. Repeat steps 3 and 4 until the grout has become too thick to test.
7. Plot shear stress vs. time for each sample. The maximum point on this plot is the yield stress.

This test was conducted on grouts C45 and PT1-1. Ideally, if shear stress is plotted against time, the curve should exhibit a well-defined yield point. This point is taken as the yield stress of the grout (Amziane and Ferraris 2007). An idealized plot of the stress growth test is shown in Figure 7-3.

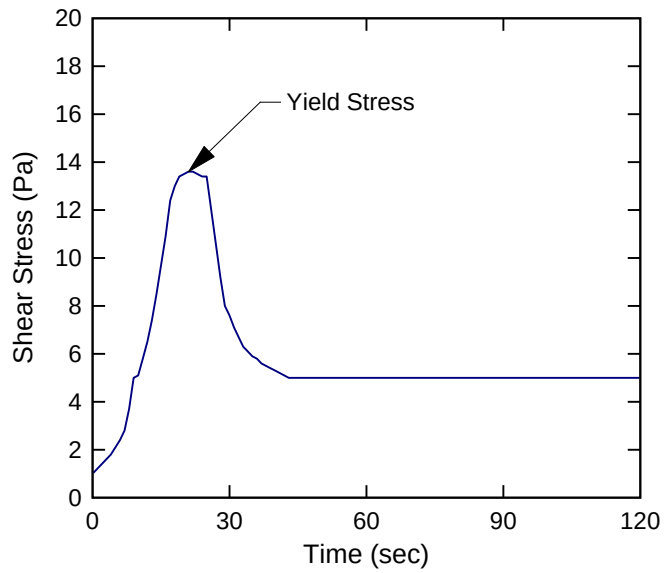

Figure 7-3. Idealized plot of stress growth test showing yield point.

Figure 7-3 shows that the measured shear stress in the grout increases initially, and then exhibits a well-defined yield point after approximately 20 seconds. Prior to yielding, the grout behaves in an elastic manner. After yielding, the grout becomes plastic and begins to flow.

Results of the stress growth test for grout C45 and grout PT1-1 are shown in Figure 7-4 and Figure 7-5 respectively.

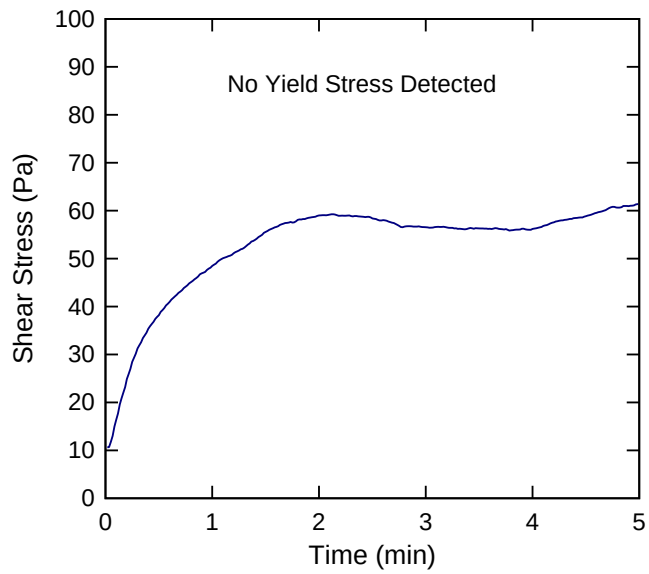

Figure 7-4. Plot of shear stress vs. time for grout C45. Tested using cup and ribbon with shear rate of 0.1 s^{-1}.

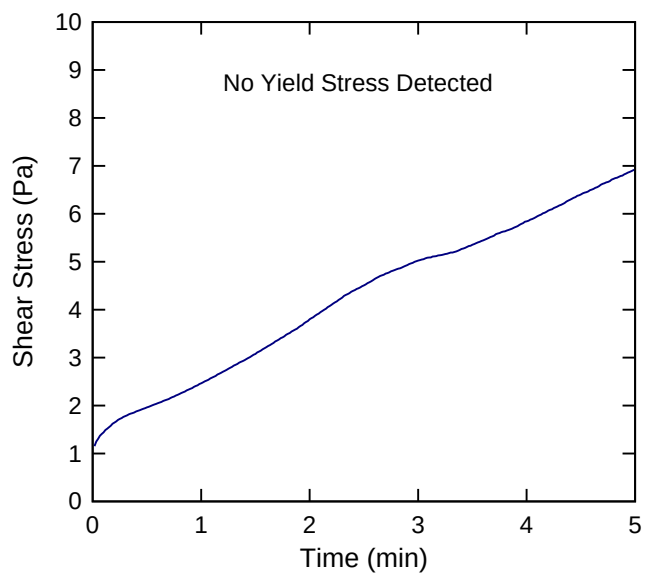

Figure 7-5. Plot of shear stress vs. time for grout PT1-1. Tested using cup and ribbon with shear rate of 0.1 s^{-1}.

The yield stress could not be measured in grout C45 or grout PT1-1 when using the cup and ribbon geometry. This is likely because, even at a very low shear rate, the cup and ribbon agitates the grout excessively and causes it to yield before the first data point is sampled. Previous researchers, such as Amziane and Ferraris (2007), were

able to measure the yield stress using the parallel plate geometry. It was not possible to use the parallel plates to test the PT grouts because of their low viscosity.

Figure 7-5 suggests that after yielding, the grout's shear stress increases with time at a low shear rate. This behavior is indicative of anti-thixotropy, which is desirable if a PT grout is nearly at rest.

The stress growth test is not a suitable replacement test for the flow cone test because it cannot be used to assess the rheological properties of the grouts using the cup and ribbon geometry. The test uses the yield stress as a metric for comparison, but the grouts tested did not exhibit a well-defined yield point.

7.4 Oscillatory Time Sweep Test

Previous researchers made use of the oscillatory test to assess the rheological properties of cement pastes and grouts with SCM in their elastic range. In this test method, the rheometer imposed an oscillating strain on the grout and measured the response strain of the grouts. The difference between the input and output strain signals was used to quantify the storage modulus, G', and the loss modulus, G". As the stiffness of the grout increased due to cement hydration, the storage modulus increased because the grouts became more solid-like. The oscillatory time sweep test method provided a way of measuring how the grout thickens over time without imposing enough shear to cause the grout to yield. This allowed for the testing of a single sample of the grout in the rheometer continuously.

The amplitude of the strain that the rheometer imposes on the grout must be in the grout's Linear-Viscoelastic Region (LVR), prior to the yield point. Similar materials (i.e. all grouts) should have similar LVRs. To determine the LVR, an oscillatory strain sweep was used. The procedure for determining the LVR was as follows:

1. Set the Peltier Jacket temperature to 90°F.
2. Mix grout according to the mix procedure in high shear mixer or blender mixer. The grout materials are stored at room temperature.
3. Perform equilibration for three minutes. This ensures the grout is at equilibrium before testing begins.
4. The rheometer imposed an oscillating strain on the grout between 0.001 and 10 in a logarithmic manner at a frequency of 1 Hz. 10 points were sampled per decade.
5. Plot G' and G" vs. Strain using logarithmic scales. G' and G" are calculated by the rheometer.
6. The flat region on the G' and G" curves provides an approximate range of the LVR.

Once the LVR of the grout was determined, a strain amplitude within the LVR was selected for the oscillatory time sweep. The procedure for the oscillatory time sweep was as follows:

1. Set the Peltier Jacket temperature to 90°F.
2. Perform equilibration for three minutes.
3. Impose a shear rate of 100 s^{-1} for a period of 1 minute to break down any structure the grout has built.
4. Impose an oscillating strain within the LVR at a frequency of 1 Hz until the grout begins to set several hours later. Sampling time = 5 seconds.
5. Plot G' vs. time.

This test was conducted on grouts C45, PT1-1, and PT2-1. Plots of the procedure used to determine the LVR for each type of grout are shown in Figure 7-6, Figure 7-7, and Figure 7-8. A summary of the LVR for each grout is provided in Table 7-2.

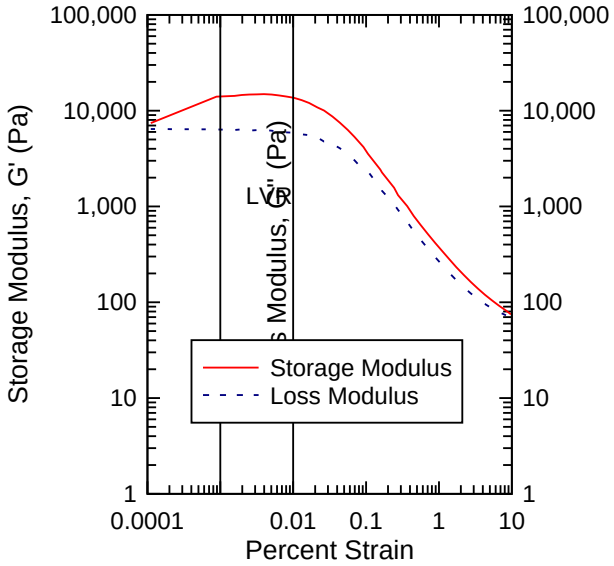

Figure 7-6. Plot of G' and G" vs. strain for grout C45.

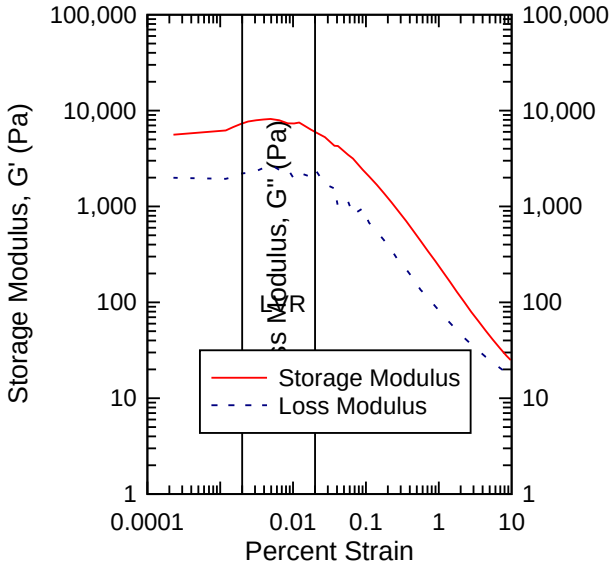

Figure 7-7. Plot of G' and G" vs. strain for grout PT1-1.

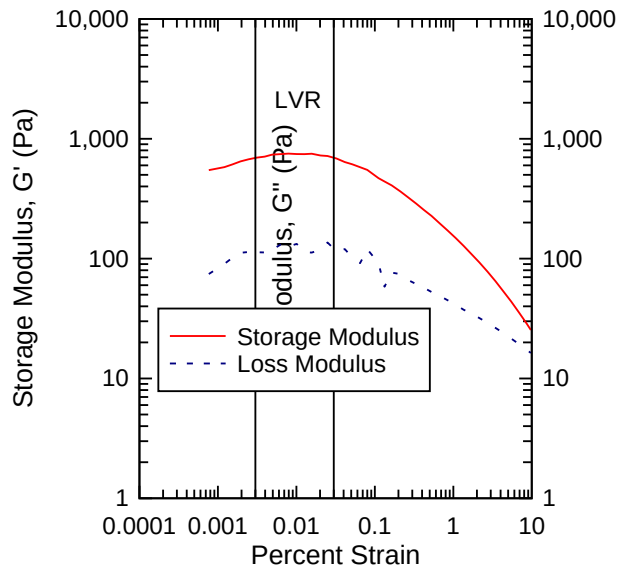

Figure 7-8. Plot of G' and G" vs. strain for grout PT2-1.

Table 7-2. Summary of LVR for each type of grout.

Grout	LVR minimum	LVR maximum
C45	0.00001	0.0001
PT1-1	0.00002	0.0002
PT2-1	0.00003	0.0003

After the LVR was determined for each grout, an oscillatory time sweep test was run on each type of grout for varying lengths of time. A strain amplitude of 0.00004 was selected. Research by Schultz & Struble (1993) indicated that the critical strain for cement paste was approximately 0.0001. This agrees well with the results presented here.

A plot of the storage modulus vs. time for each of the grouts tested is shown in Figure 7-9. This test provides a method to accurately analyze how the grouts thicken over time where they are strained in the elastic region.

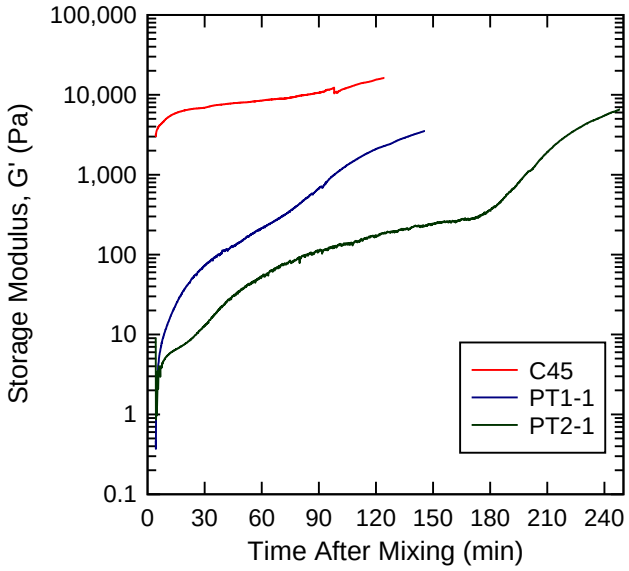

Figure 7-9. Plot of storage modulus vs. time for all tested grouts.

It can be seen that the PT grouts exhibit a larger increase in storage modulus during the first hour than the plain grout does. However, the storage modulus of the PT grouts is still much lower than that of the plain cement grout. Schultz & Struble (1993) indicate that the storage modulus of the cement paste at the critical strain was approximately 14 to 24 kPa. This agrees with the results presented here.

The oscillatory test is useful for assessing the change in stiffness of the grouts where they are in the elastic range below their yield point. This research is aimed at studying the fluidity of the grouts, which occurs in the plastic region after the grouts have yielded. The oscillatory test does not assess the plastic properties of the grouts after they have yielded, so it is not useful to assess fluidity.

CHAPTER 8
APPARENT VISCOSITY TEST

Three currently available test methods were reviewed to determine if one of them would provide a suitable replacement for the HTGF test. These were the flow curve test, the stress growth test, and the oscillatory time sweep test. Each of these tests was found to be inadequate to compare the rheological properties of plain grouts and PT grouts. The flow curve test could not be used because the Bingham model could not be applied to all of the PT grouts. The stress growth test could not be used because the grouts did not exhibit a well-defined yield point. The oscillatory time sweep test was deemed to be unsuitable because it assessed the elastic properties of the grout, not the fluid properties.

Apparent viscosity is the viscosity of a non-Newtonian fluid at a nominal shear rate. Non-Newtonian fluids exhibit different viscosities at different shear rates, so it follows that the apparent viscosity of a non-Newtonian fluid is a function of the applied shear rate. The apparent viscosity of grout was mentioned in the literature by Khayat & Yahia (1998) and Amziane & Ferraris (2007). Both reports mentioned that the apparent viscosity over a range of shear rates seemed to provide an indication of the fluidity of the grout. Neither paper provided an explicit test method for determining apparent viscosity.

A general procedure which we developed for determining the apparent viscosity was:

1. Load a sample of grout into the DSR.
2. Subject the grout to the high pre-shear rate for 30 seconds to remove the effects of inconsistent shear histories during loading.
3. Subject the grout to the *testing shear rate* for the *testing time*. The apparent viscosity is the viscosity measured at the end of the testing time.

4. Clean the grout out of the DSR.

This test was named the apparent viscosity test. For the purposes of this research, the apparent viscosity test should simulate the fluidity measurement from the flow cone test as closely as possible. Appropriate parameters were selected for the testing shear rates and testing time that simulated the flow cone test and allowed for an assessment of the fluid grout behavior at high temperatures.

8.1 Testing Shear Rate

The apparent viscosity is the viscosity of a non-Newtonian fluid evaluated at a nominal shear rate. Each of the grouts was a non-Newtonian fluid and each exhibited different behavior at different shear rates. The ideal testing shear rate for the apparent viscosity test should allow for the comparison of grouts in the same manner as the flow cone test.

A continuously varying range of shear rates are imposed on the grout in the nozzle of the flow cone during the flow cone test. The shear rate is dependent upon the viscosity of the grout and the geometry of the nozzle. The shear rate reduces as the pressure head of the grout above the nozzle drops. It was therefore necessary to investigate the grout behavior over a range of shear rates to determine empirically if a single shear rate could simulate the flow cone measurement.

Khayat & Yahia (1998) conducted an analysis to determine a relationship between flow cone time and apparent viscosity. They determined the apparent viscosity of a grout sample at several shear rates while simultaneously running the flow cone test. They showed that a shear rate of 340 to 510 s^{-1} provided a good relationship between flow cone time and apparent viscosity. The flow cone that they used had a

small nozzle of approximately 0.18 inches. The shear rate in the nozzle of their flow cone was calculated to be 375 s^{-1} using Equation 7-1.

We conducted a similar analysis to determine a relationship between apparent viscosity and the flow cone time measured in the 1/2” flow cone nozzle that we used. The shear rate in the ½” flow cone nozzle that we used was calculated to be 165 s^{-1}. Because the ½” flow cone imposed a lower shear rate on the grout, a lower range of shear rates were investigated than those Khayat & Yahia (1998) considered. Shear rates from 0 to 165 s^{-1} were investigated.

To determine a relationship between apparent viscosity and flow cone time, simultaneous flow cone and flow curve tests were run multiple times on all of the grouts. Figure 8-1, Figure 8-2, Figure 8-3, Figure 8-4, Figure 8-5, and Figure 8-6 show the apparent viscosity plotted against the flow cone time measured for the same grout sample at a shear rate of 5 s^{-1}, 25 s^{-1}, 50 s^{-1}, 75 s^{-1}, 100 s^{-1}, and 165 s^{-1} respectively. Results for all of the grouts are included in each of the plots. Table 8-1 contains a summary of trend-lines fitted to the data in each of these plots.

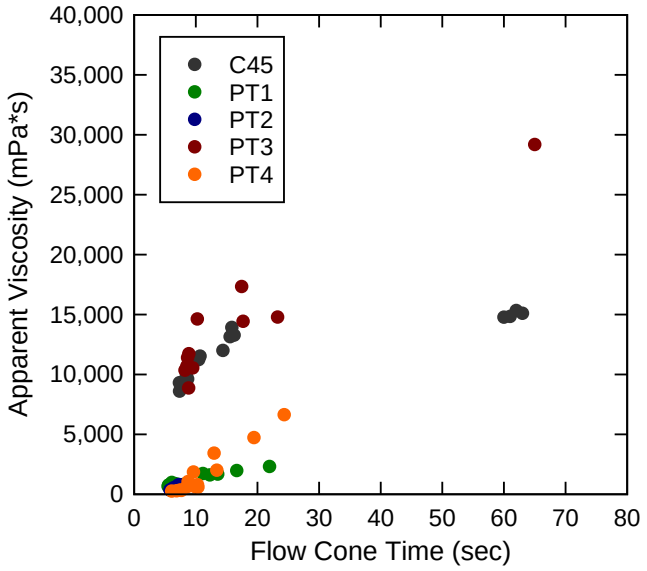

Figure 8-1. Plot of DSR viscosity versus flow cone time for DSR testing shear rate of 5 s^{-1}.

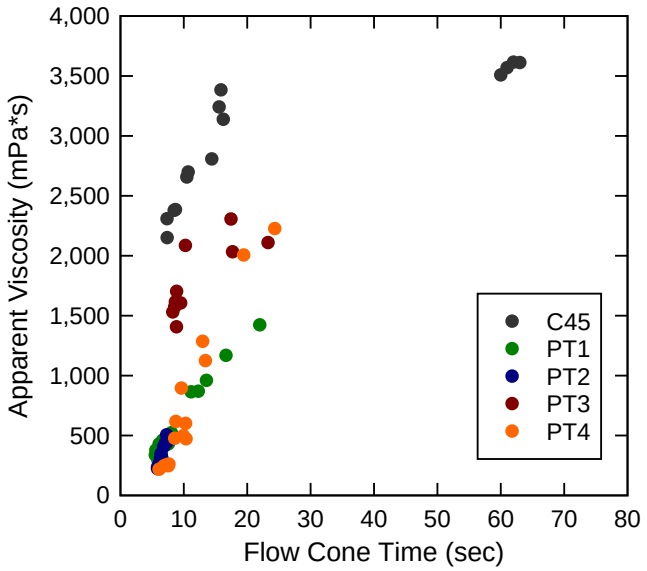

Figure 8-2. Plot of DSR viscosity versus flow cone time for DSR testing shear rate of 25 s^{-1}.

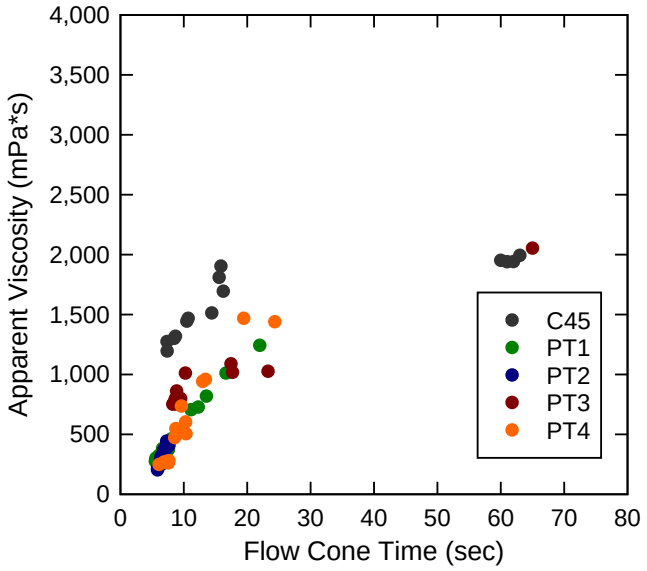

Figure 8-3. Plot of DSR viscosity versus flow cone time for DSR testing shear rate of 50 s^{-1}.

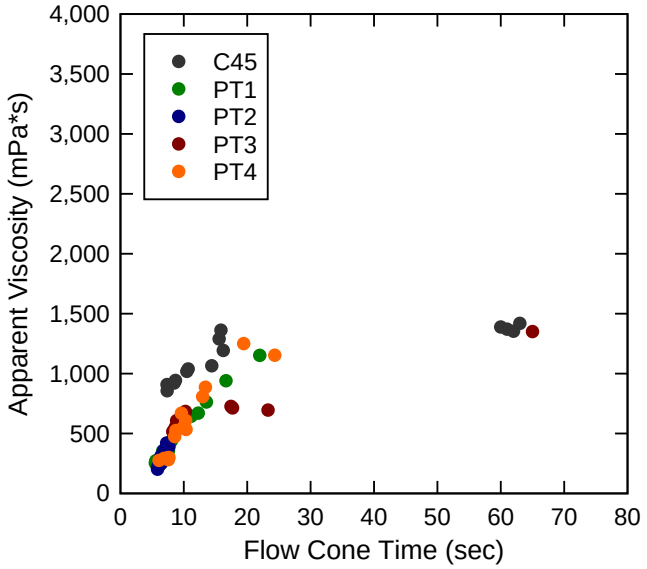

Figure 8-4. Plot of DSR viscosity versus flow cone time for DSR testing shear rate of 75 s^{-1}.

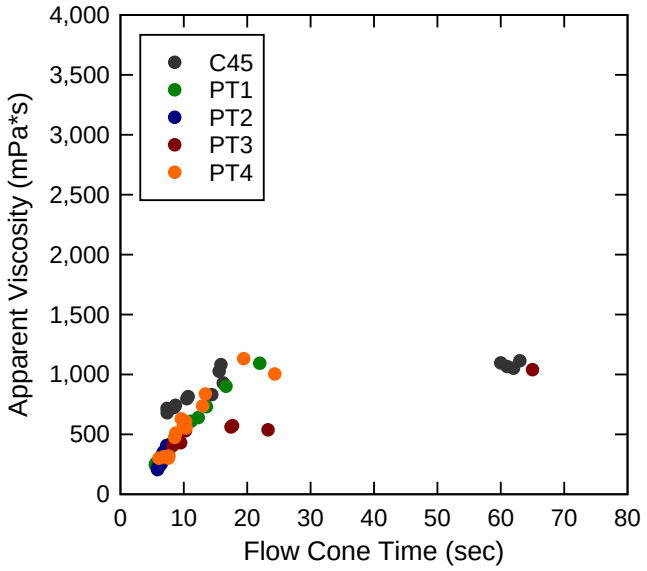

Figure 8-5. Plot of DSR viscosity versus flow cone time for DSR testing shear rate of 100 s^{-1}.

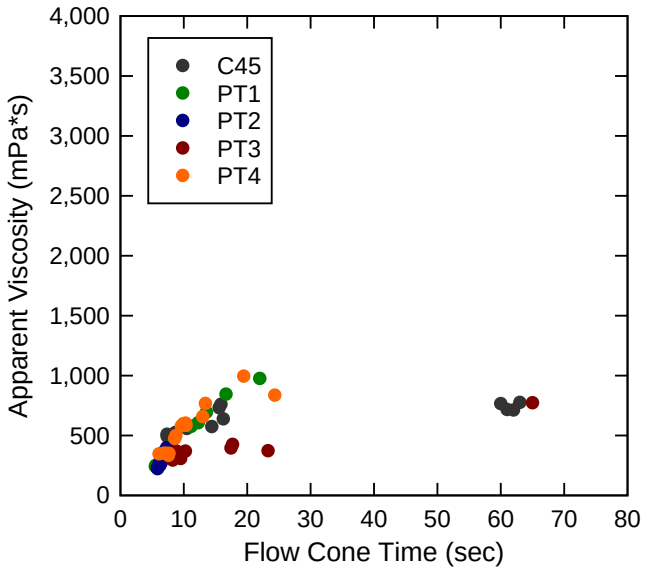

Figure 8-6. Plot of DSR viscosity versus flow cone time for DSR testing shear rate of 165 s^{-1}.

Table 8-1. Summary of R^2 values for linear trend-line fit to apparent viscosity versus flow cone time results at different shear rates.

Shear rate	R^2 PT grouts	R^2 all grouts
5 s^{-1}	0.52	0.44
25 s^{-1}	0.70	0.54
50 s^{-1}	0.71	0.55
75 s^{-1}	0.61	0.53
100 s^{-1}	0.51	0.49
165 s^{-1}	0.35	0.35

Table 8-1 shows that the best linear trend exists between flow cone time and apparent viscosity when the shear rate is either 25 s^{-1} or 50 s^{-1}.

At a low shear rate, such as 5 s^{-1} or 25 s^{-1}, as indicated in Figure 8-1 and Figure 8-2, grout PT3 exhibits a much higher apparent viscosity than the other PT grouts at the same flow cone times. A shear rate of 25 s^{-1} or less does not allow for the comparison of PT grouts in the same manner as the flow cone test. At a shear rate of 75 s^{-1} or higher, as shown in Figure 8-4, Figure 8-5, and Figure 8-6, the apparent viscosity of a grout that passes the flow cone test at approximately 20 seconds is nearly identical to the apparent viscosity of a grout that fails the flow cone test at over 60 seconds. Using a shear rate of 75 s^{-1} or higher for the apparent viscosity test makes it difficult to distinguish between a passing grout and a failing grout in the flow cone test.

At a shear rate of 50 s^{-1}, as shown in Figure 8-3, all of the PT grouts exhibit the best linear trend when comparing the apparent viscosity to the flow cone time. Grout PT3 does not quite follow this trend, but the thixotropic and shear-thinning nature of the grout causes a variation in flow cone time measurement. At this shear rate there is a distinction in apparent viscosity between the PT grouts with a flow cone time less than 30 seconds and those with a flow cone time greater than 30 seconds. The plain grouts do not follow the trend of the PT grouts at this shear rate. However, where the flow cone times were the same, the plain grouts were observed to appear more viscous than the

PT grouts. Previous research by Roussel and Le Roy (2005) showed that materials with very different apparent viscosities could exhibit similar flow cone times. For this reason, the apparent viscosity test provides a more accurate measure of the fluidity of a grout than the flow cone test does.

A testing shear rate of 50 s^{-1} is the most appropriate for the apparent viscosity test to simulate the flow cone test. This shear rate results in a very similar apparent viscosity for all of the PT grouts at a nominal flow cone time. It also allows for a quantitative distinction between grouts that pass the flow cone test and grouts that fail the flow cone test. A pre-shear rate of 165 s^{-1} was selected to eliminate inconsistencies in the shear history of the grout during loading.

8.2 Testing Time

The time domain for the apparent viscosity test is critical. All of the grouts exhibit varying degrees of thixotropy and anti-thixotropy, meaning that their viscosity will change over time if they are subjected to a constant shear rate, as they are in the apparent viscosity test. Some grouts exhibit both thixotropy and anti-thixotropy, depending on the time domain over which they are tested. Figure 8-7 contains the results of a 60-minute apparent viscosity test run on grouts C45, PT1-1, PT2-1, PT3-1, and PT4-1. Grout PT1-1, PT2-1, and PT3-1 were mixed at the manufacturer's maximum specified water content. Grout PT4-1 was mixed at the mid-range of the manufacturer's specified water content.

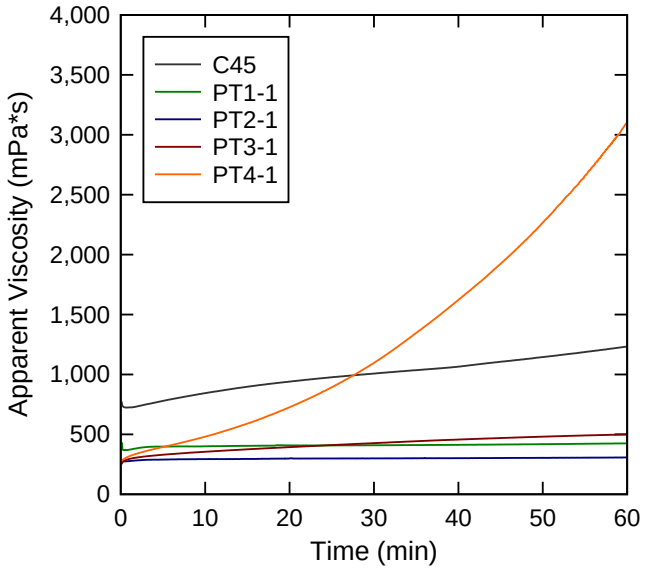

Figure 8-7. Results of 60-minute apparent viscosity test conducted on grouts C45, PT1-1, PT2-1, PT3-1, and PT4-1.

The initial apparent viscosity of grout C45 is approximately 750 mPa*s. After 30 minutes of testing, however, the apparent viscosity is approximately 1,000 mPa*s. This is an indication that, at a shear rate of 50 s^{-1}, grout C45 is anti-thixotropic, because its apparent viscosity increases over time when subjected to a constant shear rate. Grout PT4-1 exhibits anti-thixotropy to a greater degree than grout C45. Grout PT3-1 exhibits a small degree of anti-thixotropy at a shear rate of 50 s^{-1} as well. Grouts PT1-1 and PT2-1 exhibit a nearly constant apparent viscosity throughout the 60-minute testing period. This is a good indication that, at a shear rate of 50 s^{-1}, grouts PT1-1 and PT2-1 are not thixotropic or anti-thixotropic.

The results of the first 5 minutes of the apparent viscosity tests that are shown in Figure 8-7 are given in Figure 8-8.

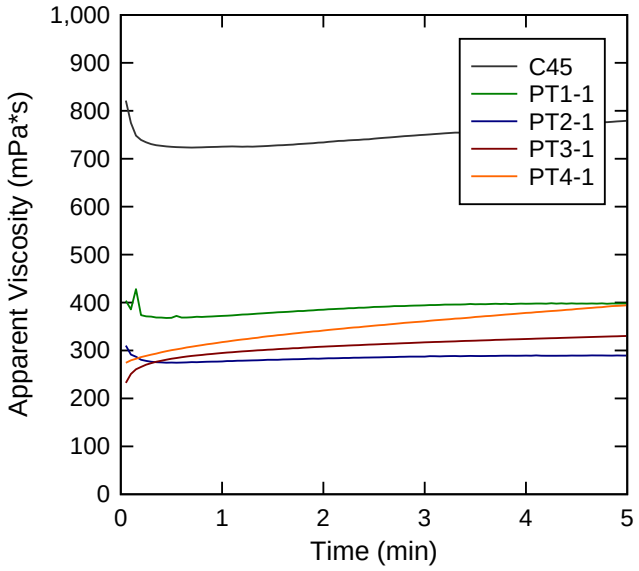

Figure 8-8. Results of first 5 minutes of apparent viscosity test conducted on grouts C45, PT1-1, PT2-1, PT3-1, and PT4-1.

Each of the grouts exhibits some thixotropy or anti-thixotropy over the first 15 seconds of testing. Grout C45 is initially thixotropic, before later exhibiting anti-thixotropy. Grouts PT3-1 and PT4-1 both exhibit anti-thixotropy in this time domain. Grouts PT1-1 and PT2-1 do not exhibit a large degree of thixotropy or anti-thixotropy.

A test length of 1 minute is comparable to the total time it takes to run one flow cone test. At 1 minute, the viscosities of grouts C45, PT3-1, and PT4-1 are in the middle of an increasing trend. Figure 8-7 showed that the viscosity of these materials will continue to increase for at least 60 minutes. The apparent viscosity after 1 minute negates the large effects of thixotropy in the first 15 seconds. A 1-minute test also allows for testing to be completed in a reasonable amount of time without significant effects on the results. For these reasons, the apparent viscosity test should be run for 1 minute to simulate the flow cone measurement.

8.3 Summary

Apparent viscosity, which is the viscosity of a non-Newtonian fluid, was mentioned by previous grout researchers Khayat & Yahia (1998) and Amziane & Ferraris (2007). No explicit test method was given. We selected parameters for the testing shear rate and testing time for the apparent viscosity test that allowed for a simulation of the flow cone test.

The following variables allow for the most direct relationship between flow cone time and apparent viscosity for the PT grouts:

- Testing Shear Rate: 50 s^{-1}
- Testing Time: 1 minute

The apparent viscosity test can be used to simulate the flow cone test. The test results in the measurement of a similar viscosity for the PT grouts at a nominal flow cone time. The finalized procedure for the apparent viscosity test is as follows:

1. Load a sample of grout into the DSR.
2. Subject the grout to a shear rate of 165 s^{-1} for 30 seconds.
3. Subject the grout to a shear rate of 50 s^{-1} for a period of 1 minute, sampling every 1 second. The apparent viscosity is the viscosity measured at 1 minute.
4. Clean the grout out of the cup and ribbon.

CHAPTER 9
HIGH TEMPERATURE GROUT FLUIDITY TEST

The HTGF test was used in the past by FDOT to determine whether or not a grout would remain pumpable under simulated hot weather conditions. The test was run by mixing a batch of grout using the colloidal mixer. The grout materials and equipment were conditioned in a 90°F environment for at least 18 hours prior to initiating the test. After mixing, the grout was continuously pumped through 400 ft. of hose, also in the conditioned environment, for a period of 60 minutes. The 60-minute conditioning period began when the grout had fully re-circulated through the 400 ft. of hose. Flow cone times were measured every 15 minutes to check the fluidity of the grout. The grout was considered to pass the test if the flow cone times were less than 30 seconds at every point during testing. A general procedure for the HTGF test was given by FDOT (2007). The procedure was as follows:

1. Mix grout in colloidal grout plant according to mix procedure. Grout plant and grout materials are stored in conditioned environment. See Figure 9-1 and Figure 9-2.
2. Transfer grout to agitation tank and start agitator paddle. See Figure 9-3.
3. Pump grout from agitation tank through 400 ft. of 1-in grout hose which returns to agitation tank. See Figure 9-4.
4. Continue re-circulating grout for 60 minutes. Maintain flow rate between 0.1 and 0.25 gal/sec, per PTI specifications (Post-Tensioning Institute 2012).
5. Draw a sample at the following times after re-circulation is complete: 0 minutes, 15 minutes, 30 minutes, 45 minutes, and 60 minutes. Record the following for each sample: ambient temperature, grout temperature, pumping pressure, hose flow rate, flow cone time, mud balance specific gravity, and unit weight.
6. Every time a sample is collected, use the DSR to run the apparent viscosity test.

Figure 9-1. Environmental chamber used for temperature control during HTGF testing. Photo courtesy of Trey Hamilton.

Figure 9-2. Inside of environmental chamber used for temperature control during HTGF testing. Photo courtesy of Trey Hamilton.

Figure 9-3. Transfer grout to agitation tank and start agitator paddle. Photo courtesy of Trey Hamilton.

Figure 9-4. Return grout to agitation tank after pumping through 400 ft. of hose. Photo courtesy of Trey Hamilton.

The sampling procedure for the HTGF test is as follows:

1. Collect 2-3 gallon sample from the return end of the 400 ft. of hose into a 5-gallon bucket. See Figure 9-5.

2. With 10 seconds of running the flow cone test, shear the grout in the 5-gallon bucket using a paint-paddle style agitator. See Figure 9-6.

3. Collect samples for the other tests from the flow cone discharge.

Figure 9-5. Collect 2-3 gallon sample from return end of 400 ft. of hose into 5-gallon bucket. Photo courtesy of Trey Hamilton.

(a) (b)

Figure 9-6. Paint paddle style agitator (a) and blades (b) used to shear grout within 10 seconds of flow cone testing. Photos courtesy of Trey Hamilton.

9.1 Flow Cone Test

The flow cone is typically used in the field to measure the fluidity of freshly mixed grout. Figure 9-7 shows the flow cone test being setup during the HTGF test. The flow cone test was run on each grout sample collected during the HTGF test.

Figure 9-7. Flow cone used to determine fluidity of grout samples during HTGF testing. Photo courtesy of Trey Hamilton.

The flow cone test procedure is a modified version of ASTM C939 (2010). The procedure for running the flow cone test is as follows:

1. Fill flow cone with water.
2. One minute or less before introducing the grout, drain the water out of the flow cone and close the outlet with a rubber stopper.
3. Fill flow cone to top with grout. Place 1,000 mL cylinder below flow cone.
4. Remove the rubber stopper from the outlet and start stopwatch.
5. After 1,000 mL has drained from flow cone, stop the stop watch.
6. Record this time as the flow cone efflux time.

9.2 Mud Balance Test

The mud balance test is used in the field determine the specific gravity of a small sample of fresh grout. A mud balance is shown in Figure 9-8. The mud balance test was run on each grout sample collected during the HTGF test.

Figure 9-8. Mud balance used to determine unit weight of grout samples during HTGF testing. Photo courtesy of Trey Hamilton.

The procedure for the mud balance test was given in ASTM D4380 (2006). The procedure was as follows:

1. Pour a sample of grout into the cup on the mud balance.
2. Tap the side of the cup to ensure that air bubbles rise to surface.
3. Place the cap onto the cup. Allow grout to flow out through the hole in the cap, ensuring that the cup is totally filled.
4. Place the mud balance assembly on the fulcrum in the case.
5. Adjust the weight on the balance arm until the mud balance is level.
6. Record the specific gravity of the grout sample.

9.3 Unit Weight Test

The unit weight test was run in addition to the mud balance test to determine the unit weight of fluid samples of grout. The unit weight had a known volume of 0.0141 ft^3. The unit weight is shown in Figure 9-9. A photograph of the unit weight being filled is

shown in Figure 9-10. The unit weight test was run on each grout sample collected during the HTGF test.

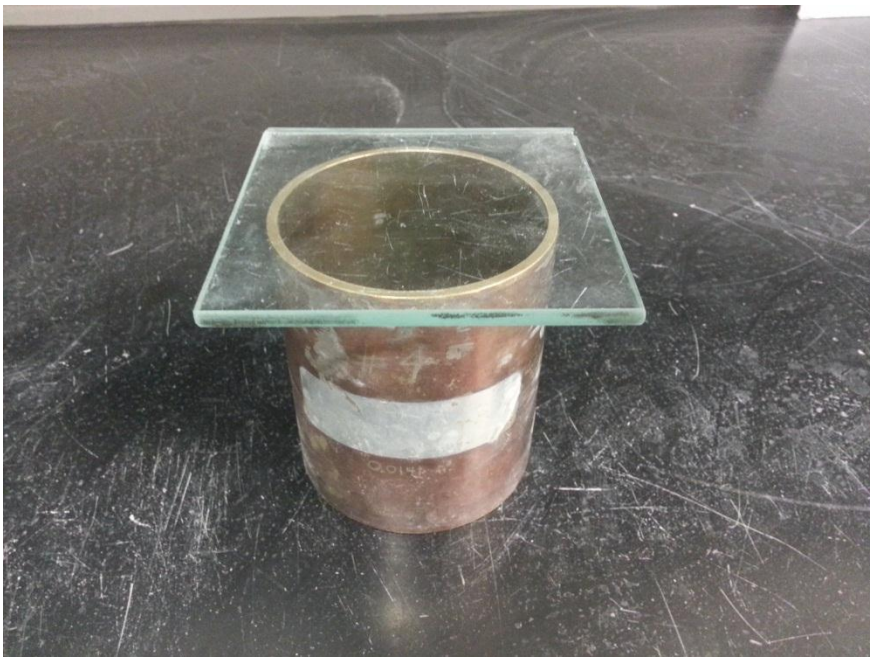

Figure 9-9. Unit weight used to determine grout density. Photo courtesy of Alex Piper.

Figure 9-10. Unit weight being filled for testing. Photo courtesy of Alex Piper.

The procedure for the unit weight test was as follows:

1. Tare the unit weight cup and glass top.
2. Fill the cup with grout (Figure 9-10). Tap the side of the cup to ensure that air bubbles rise to surface.
3. Use the glass top to screed the surface of the grout in the cup.
4. Weigh the tared cup, which is filled with grout.
5. Calculate the unit weight. Divide the weight of the grout by the volume of the cup.

CHAPTER 10
RESULTS AND DISCUSSION – HIGH TEMPERATURE GROUT FLUIDITY TEST

The HTGF test was conducted on grouts PT1-2, PT2-2, PT3-1, and PT4-1. The PT grouts were tested at both the upper limit and median point of the manufacturer's water content specifications. Results measured during the HTGF test are included in the following sections.

9.4 Flow Cone Test Results

A flow cone test was conducted every 15 minutes over the course of the HTGF test's one hour recirculation period. The variation in flow cone time with respect to recirculation time for all tests is shown in Figure 10-1.

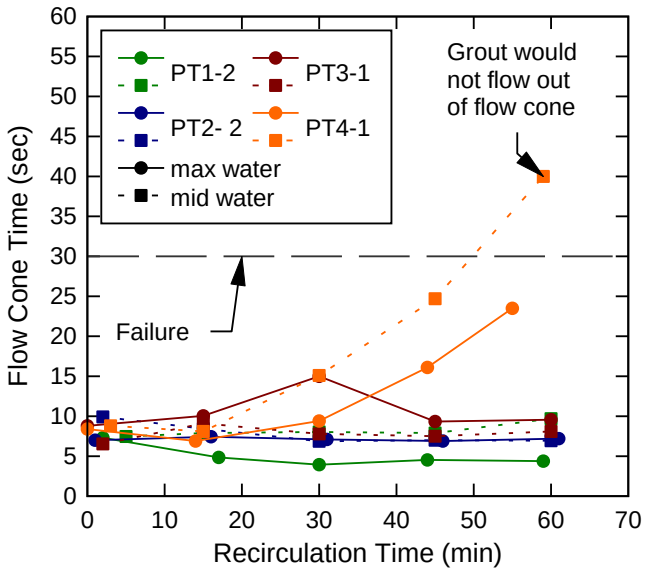

Figure 10-1. Plot of flow cone results versus recirculation time for all HTGF tests.

With the exception of grout PT4-1, the PT grouts maintained flow cone efflux times of less than 15 seconds. Grout PT3-1 at maximum water exhibited a single high flow cone time at the 30-minute sampling time but then returned to less than 15 sec for the subsequent two tests. Due to the shear-thinning and thixotropic properties of grout PT3-1, the time between collecting a sample and running the flow cone test had a major impact on the measured flow cone time. This is likely the source of the single high flow

cone time in grout PT3-1 at maximum water. Grout PT4-1 showed an increasing trend for both maximum and mid-range water addition rates, with the mid-range water test failing. The last sample taken from PT4-1 during the mid-range test would not flow out of the flow cone, which caused it to fail the HTGF test.

9.5 Apparent Viscosity Test Results

The DSR was used to run the apparent viscosity test to assess the grout fluidity during the HTGF test. Apparent viscosity tests were conducted every 15 minutes during the recirculation period. The variation in apparent viscosity with respect to recirculation time for all of the samples tested is shown in Figure 10-2.

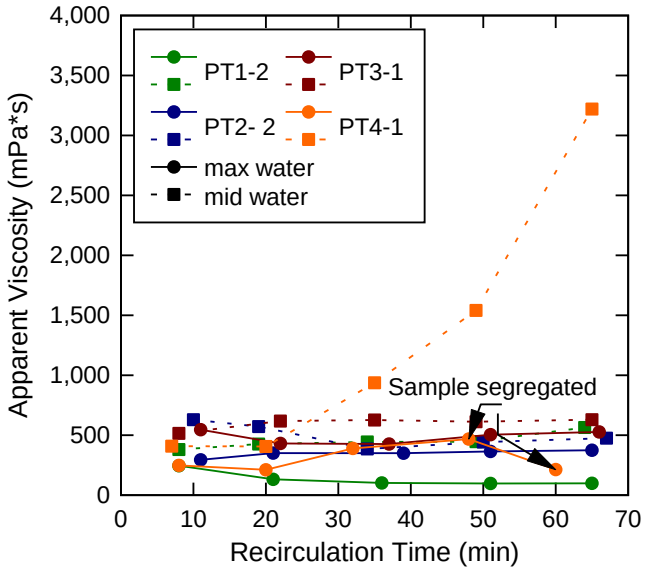

Figure 10-2. Plot of DSR apparent viscosity versus recirculation time for all HTGF tests.

The apparent viscosity curves display a similar trend to the flow cone curves for each grout in nearly every case. Grouts PT1-2, PT2-2, and PT3-1 each exhibited relatively low and constant apparent viscosities during the entire recirculation period at both their maximum and mid-range water content. These results are similar to the flow cone test results. At mid-range water content, grout PT4-1 exhibited a significant increase in apparent viscosity over the one hour testing period, as it did during the flow

cone test. When grout PT4-1 was tested at its maximum water content, issues were noted when running the DSR test at the 45-minute and 60-minute sampling times. The samples loaded into the DSR cup had segregated and contained excessive water, resulting in the measurement of a very low apparent viscosity. Therefore, the data measured at the 45-minute and 60-minute sampling points on grout PT4-1 at maximum water content are not valid.

9.6 Temperature Results

The ambient temperature and grout temperature were measured every time a sample was collected during the HTGF test. Figure 10-3 contains a plot showing the variation in ambient temperature and grout temperature with respect to recirculation time for each HTGF test. Table 10-1 contains a summary of the ambient temperatures, grout temperatures, and difference between grout temperature and ambient temperature that were measured during the HTGF test.

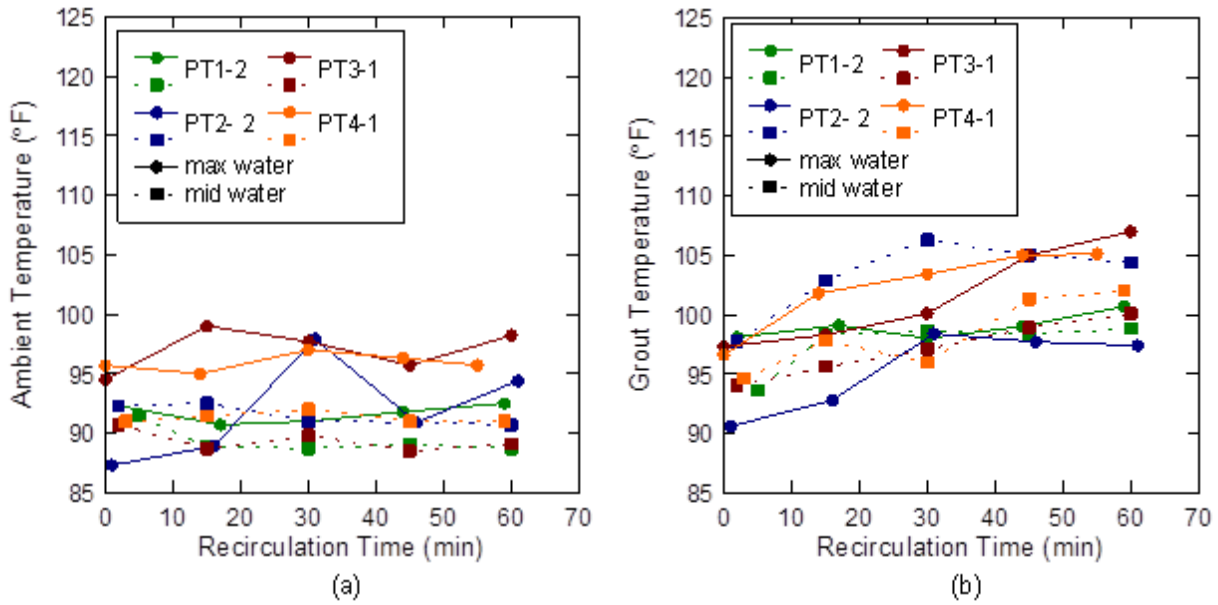

Figure 10-3. Plot of ambient temperature (a) and grout temperature (b) versus recirculation time for all grouts tested in HTGF test.

Table 10-1. Summary of ambient and grout temperatures measured during HTGF test.

Grout	Water	Ambient temperature (°F)			Grout temperature (°F)			Difference (°F)		
		High	Low	Avg	High	Low	Avg	High	Low	Avg
PT1-2	Max	93	91	92	101	98	99	8	6	7
	Mid	91	89	89	99	94	98	10	2	8
PT2-2	Max	98	87	92	98	91	95	7	1	4
	Mid	93	91	91	106	98	103	15	5	12
PT3-1	Max	99	95	97	107	97	102	9	-1	5
	Mid	91	89	89	100	94	97	11	3	8
PT4-1	Max	97	95	96	105	97	102	9	1	6
	Mid	92	91	91	102	95	98	11	4	7
Totals		99	87	92	107	91	99	15	-1	7

The target ambient temperature was 90°F. Several of the batches exhibited a higher ambient temperature because it was difficult to precisely control the temperature of the environmental chambers used for testing. In all cases, the ambient temperature was fairly constant throughout the testing period.

Although the test is intended to run at an ambient temperature of 90°F, the temperatures of the grouts were on average 7°F higher than ambient. When the HTGF test was run on grout PT2-2 at mid-range water content, the grout temperature was 15°F higher than ambient in one case.

9.7 Pressure and Flow Rate Results

At the sampling intervals during grout recirculation, grout pressure at the pump outlet and grout flow rate at the discharge end of the 400 ft. recirculation hose were recorded. A plot showing the variation in pumping pressure and grout flow rate during the course of recirculation is given in Figure 10-4. Note that the pumping pressure was not recorded during all of the HTGF tests.

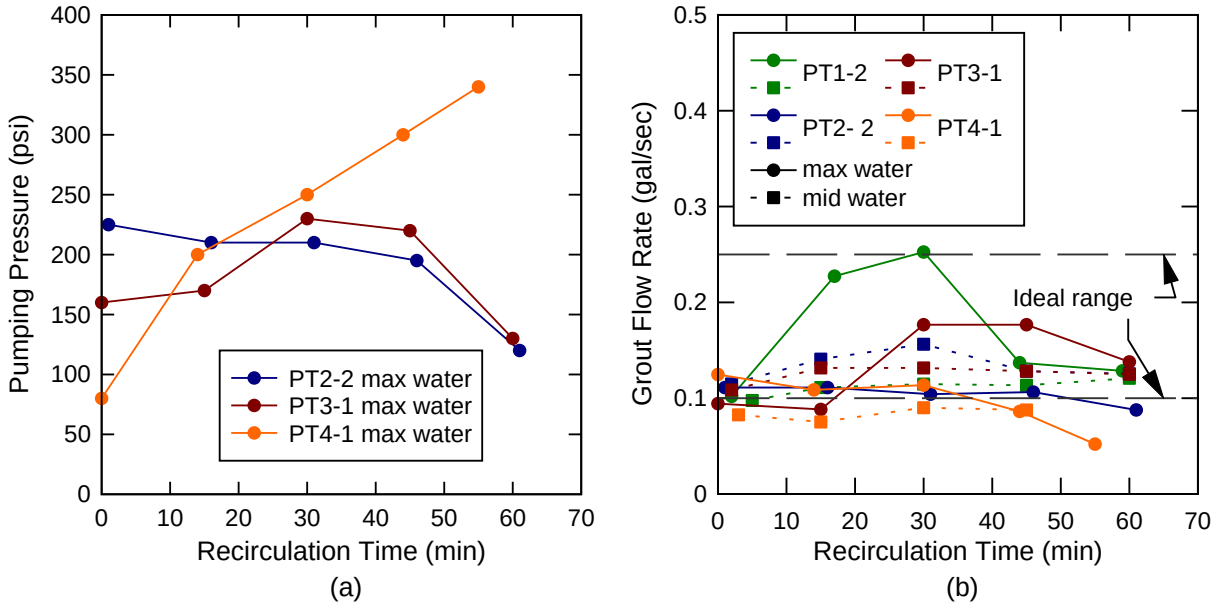

Figure 10-4. Plot of pumping pressure (a) and grout flow rate (b) versus recirculation time for all grouts tested in HTGF test.

During testing, the flow rate was adjusted to stay within the limits set forth by PTI (Post-Tensioning Institute 2012). These limits are indicated in Figure 10-4 (b). The pumping pressure was adjusted to increase or decrease the flow rate of the grout through the 400 ft. of hose.

In nearly all cases, the flow rate of the grout through the 400 ft. of hose was within the limits set forth by PTI. At maximum water content for grout PT4-1, very high pumping pressures were used to attempt to maintain the flow rate. However, due to the high viscosity of the grout, it was not possible to maintain the flow rate within PTI's limits.

FDOT states that normal pumping pressure should be between 10-50 psi (FDOT 2002) while PTI states that pumping pressures should be less than 145 psi (Post-Tensioning Institute 2012). The grouts tested during the HTGF test required much higher pressures in each case where the pressure was recorded. Although no pressure

data were recorded during PT4-1 testing at its mid-range water content, the grout had stiffened such that the grout could not be pumped out of the hose during cleanup.

9.8 Mud Balance and Unit Weight Results

The mud balance and unit weight tests were used to determine the density of the grouts during the HTGF test. Figure 10-5 shows the mud balance and unit weight values of the grout taken during the regular sampling intervals. Table 10-2 provides a summary of the initial unit weight as well as the changes in unit weight during the recirculation period.

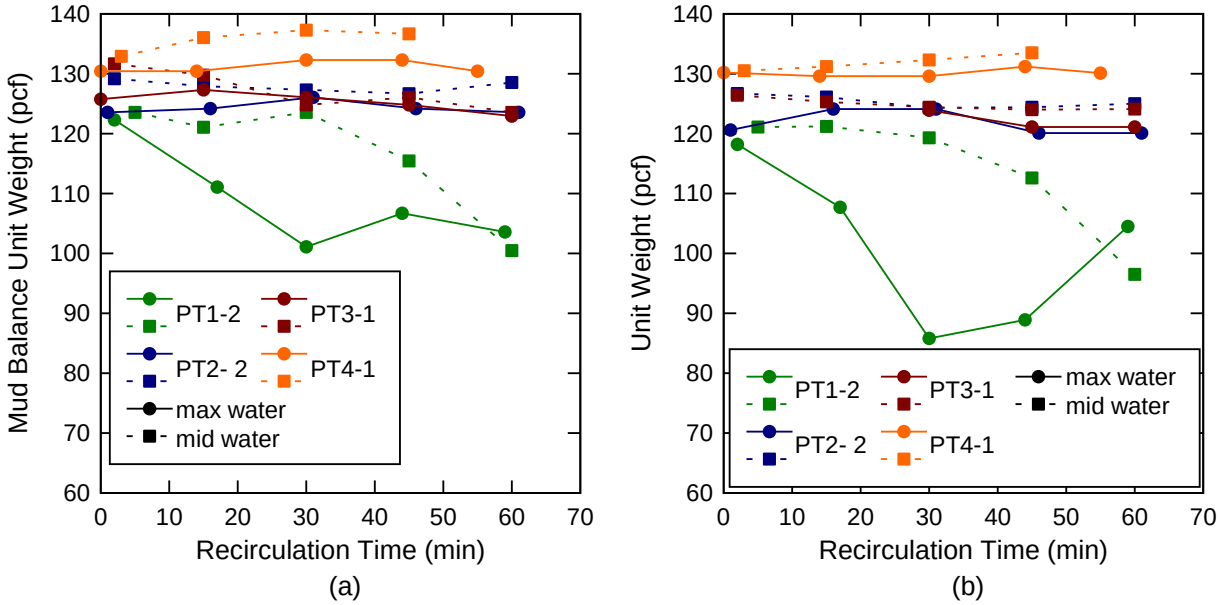

Figure 10-5. Plot of mud balance density (a) and unit weight (b) versus recirculation time for all grouts tested in HTGF test.

Table 10-2. Summary of initial unit weights as well as maximum increase and decrease in unit weight during testing.

Grout	Water	Mud balance density			Unit weight		
		Initial	Increase	Decrease	Initial	Increase	Decrease
PT1-2	Max	122.3	-	21.2	118.2	-	32.4
	Mid	123.6	-	23.1	121.1	0.1	24.6
PT2-2	Max	123.6	2.5	0.0	120.6	3.5	0.5
	Mid	129.2	-	2.5	126.7	-	2.4
PT3-1	Max	125.7	1.6	2.8	123.9	-	2.8
	Mid	131.7	-	8.1	126.4	-	2.4
PT4-1	Max	130.4	1.9	-	130.2	1.0	0.6
	Mid	132.9	4.4	-	130.5	3.0	-

With the exception of grout PT1-2, all of the grouts exhibit a fairly constant density as measured by both the mud balance test and the unit weight test. The maximum increase or decrease in unit weight during the tests on these grouts was 6.1%, which was measured using the mud balance on grout PT3-1 at mid-range water content. Grout PT1-2, however, exhibited foaming during the recirculation period, which was accompanied by a decrease in unit weight between 17% and 27%, depending on the measurement instrument.

CHAPTER 11
FLOW CONE TO APPARENT VISCOSITY CALIBRATION

To develop a DSR replacement test for the HTGF test, it was necessary to determine a limit in the apparent viscosity test at which the grouts should fail. Each time a sample was collected during the HTGF test, simultaneous flow cone and apparent viscosity tests were run. These data were compared to determine a failure limit for the apparent viscosity test.

Figure 11-1 contains a plot of apparent viscosity versus flow cone time for the samples of grout collected during the HTGF test.

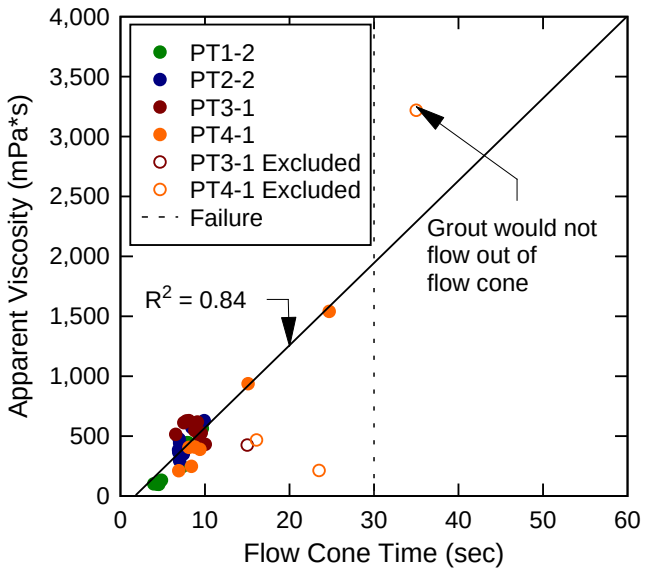

Figure 11-1. Plot of apparent viscosity versus flow cone time for samples collected during HTGF test.

A linear trend with an R^2 value of 0.84 exists between the apparent viscosity and the flow cone time of the PT grout samples tested in the HTGF test. Two of the tests conducted on grout PT4-1 are excluded from this analysis because the DSR samples contained excessive water. Another one of the samples of grout PT4-1 was excluded because the grout would not flow out of the flow cone. A sample of grout PT3-1 at

maximum water content was also excluded because of the excessively thixotropic nature of the grout, which resulted in an unusually high flow cone time.

Based on these data, a flow cone time of 30 seconds corresponds to an apparent viscosity of approximately 2,000 mPa*s. However, very little data were recorded for flow cone times above 12 seconds. All of the PT grouts tested, with the exception of grout PT4-1, exhibited low flow cone times throughout the HTGF test. Grout PT4-1 exhibited higher flow cone times, but a small amount of data were recorded because only two HTGF tests were run on each grout.

During the HTGF test, one sample of grout PT4-1 was collected that had a flow cone time of about 25 seconds and a viscosity of about 1,500 mPa*s. The grout sampled at this point could still be pumped by the grout plant, and passed the HTGF test. A majority of the PT grouts exhibited a viscosity lower than 750 mPa*s at flow cone times of less than 12 seconds in the HTGF test. Considering these data, recommended criteria for qualifying a PT grout using the apparent viscosity test based on the HTGF test are given in Table 11-1.

Table 11-1. Recommended criteria for qualifying grouts using apparent viscosity test.

Apparent viscosity result	Qualifying condition
Apparent viscosity ≤ 750 mPa*s	Grout passes.
750 mPa*s < *Apparent viscosity* ≤ 1,500 mPa*s	Cannot qualify with apparent viscosity. Run HTGF test.
Apparent viscosity > 1,500 mPa*s	Grout fails.

Apparent viscosity test results recorded during the HTGF test are given in Figure 11-2.

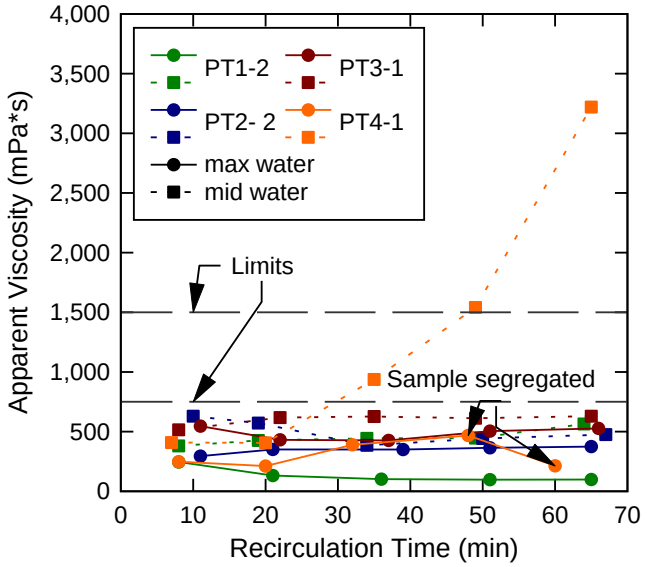

Figure 11-2. Apparent viscosity results from HTGF test with failure limits shown.

With the exception of the tests on grout PT4-1 at mid-range water content, all of the grouts passed the apparent viscosity test using the conditions given in Table 11-1. They passed because the apparent viscosity was less than 750 mPa*s throughout the HTGF 60-minute recirculation period. Grout PT4-1 at mid-range water content failed the test because the viscosity exceeded 1,500 mPa*s during the 60-minute recirculation period.

CHAPTER 12
DEVELOPMENT OF SIMULATED CONDITIONING TECHNIQUE

The HTGF test imposed a dynamic mechanical shearing action on the grout in between sampling; it was necessary to replicate this conditioning to produce the same rheological response in the grout. Although the HTGF test is initiated with the grout materials and equipment at 90°F, the energy imparted during mixing and recirculation increases the temperature of the grout by about 7°F to 15°F. Two methods were investigated to simulate the conditioning process imposed on the grout by the HTGF test. The first made use of the high shear mixer to agitate the grout in between sampling. The second made use of the DSR to agitate the grout continuously for one hour. Both of these methods are more amenable to a typical construction materials testing laboratory than the HTGF test.

9.9 Temperature

The mixing and conditioning process imposed on the grout by the HTGF test caused the grout temperature to increase approximately 7°F to 15°F higher than the ambient temperature of 90°F. A study was conducted to determine the effect of temperature on the apparent viscosity of both plain and PT grouts. The apparent viscosity test was run several times over a period of 60 minutes after mixing on both plain and PT grouts over a range of temperatures. No conditioning was performed between apparent viscosity tests; the grout was allowed to remain at rest in a vacuum-sealed container.

Figure 12-1 contains the results of the apparent viscosity test at temperatures between 75°F and 120°F for grout C45, Figure 12-2 contains similar results for grout PT1-1, and Figure 12-3 contains similar results for grout PT2-1. Note that the scale on

Figure 12-1 is greater than that on Figure 12-2 and Figure 12-3 by an order of magnitude.

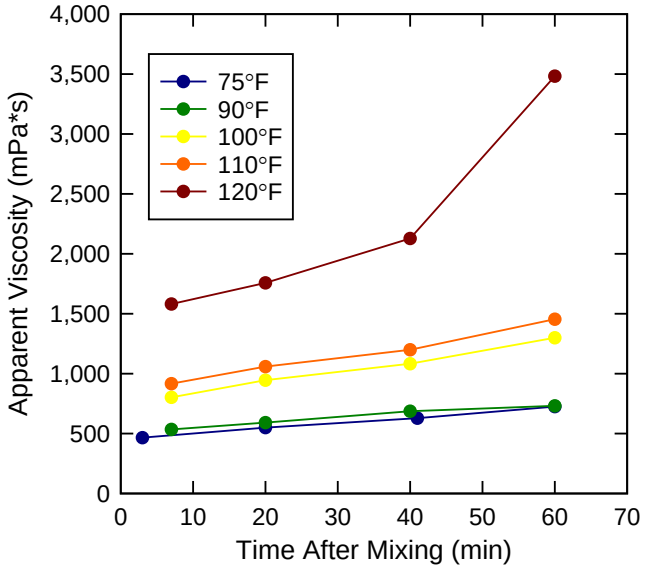

Figure 12-1. Plot of apparent viscosity vs. time after mixing for grout C45 at different temperatures with no conditioning between tests.

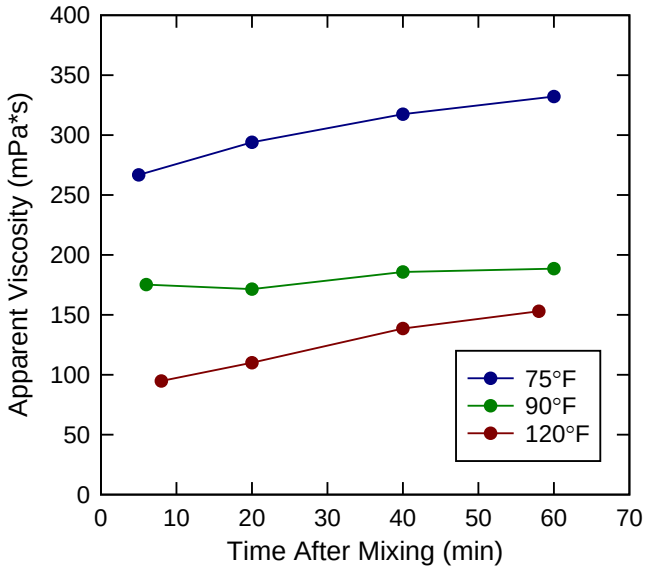

Figure 12-2. Plot of apparent viscosity vs. time after mixing for grout PT1-1 at different temperatures with no conditioning between tests.

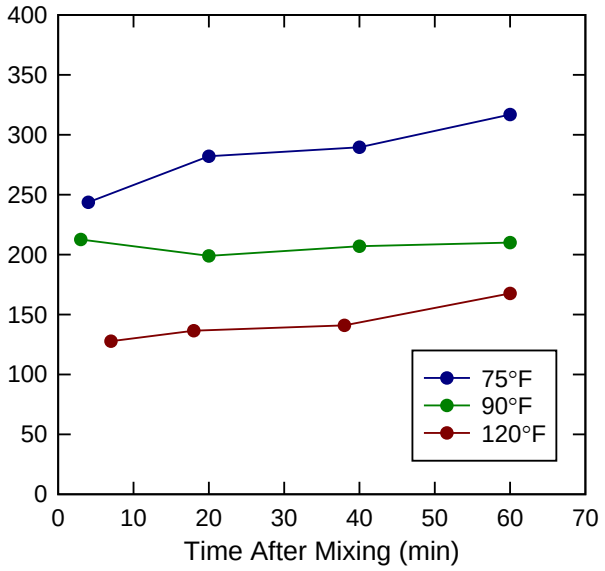

Figure 12-3. Plot of apparent viscosity vs. time after mixing for grout PT2-1 at different temperatures.

Generally, the viscosity of the plain grouts and the PT grouts increase over the course of the one hour testing period at any temperature. As the temperature is increased, the plain grouts see an increase in viscosity as well. The viscosity of the PT grouts, however, decreases as the temperature increases. These results indicate that an increase in temperature has a much larger effect on the viscosity of the plain cement grouts than it does on the viscosity of the PT grouts.

Because temperature has a significant impact on the viscosities of the different grouts, the new conditioning process should replicate the grout temperatures measured during the HTGF test.

9.10 DSR Conditioning

A series of tests were run on all of the PT grouts in which the DSR was used to condition and test the grout. Essentially, the apparent viscosity test was run on a grout sample continuously for 1 hour. The Peltier jacket on the DSR was used to control the

sample temperature during testing. The procedure used for the test in which the DSR conditioned the grout is as follows:

1. Mix grout according to the mix procedure in high shear mixer with water bath set to 100°F. The grout materials are stored at room temperature.
2. Set the Peltier jacket temperature to 100°F
3. Load a sample of grout into the DSR.
4. Subject the grout to the high pre-shear rate for 30 seconds.
5. Subject the grout to a shear rate of 50 s^{-1} for a period of 60 minutes, sampling every 1 second.
6. Plot the apparent viscosity at the following times: 1 second, 15 minutes, 30 minutes, 45 minutes, and 60 minutes.
7. Clean the grout out of the cup and ribbon.

A comparison of the apparent viscosity measured using the DSR for grout conditioning versus that measured when the HTGF test was used for conditioning is shown in Figure 12-4. Samples collected at the same mixing water content and times after mixing are compared.

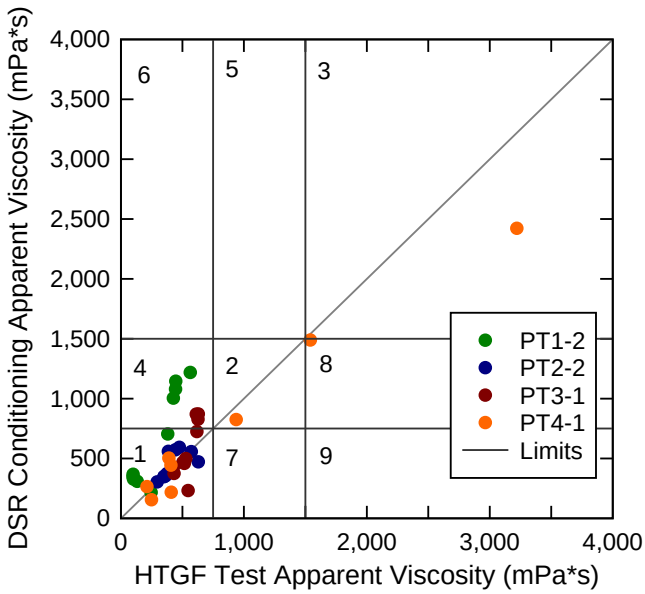

Figure 12-4. Plot of apparent viscosity measured when DSR was used for grout conditioning versus apparent viscosity measured during HTGF test.

The plot is broken into nine zones, each of which corresponds to a different set of qualifying conditions when using the HTGF test to condition the grout and when using the DSR to condition the grout. These conditions are given in Table 11-1.

Table 12-1 provides a summary of the number of samples contained in each zone. It also details the implications of each zone when using the DSR to condition the grout instead of the HTGF test. In a neutral zone, both conditioning techniques result in the same qualifying outcome. In a conservative zone, the grout is more likely to fail the apparent viscosity test when the DSR is used for conditioning than when the HTGF test is used for conditioning. In a non-conservative zone, the grout is more likely to pass the apparent viscosity test when the DSR is used for conditioning than when the HTGF test is used for conditioning. Note that the result “Cannot qualify” means that the flow cone test result from the HTGF test must be used to qualify the grout. The apparent viscosity cannot be used to qualify a grout with a viscosity between 750 mPa*s and 1,500 mPa*s.

Table 12-1. Comparison of apparent viscosity results under different conditioning techniques.

Zone	Result (DSR)	Result (HTGF)	Samples	Percentage	Status
1	Pass	Pass	28	74%	
2	Cannot qualify	Cannot qualify	1	3%	Neutral
3	Fail	Fail	1	3%	
4	Cannot qualify	Pass	7	18%	
5	Fail	Cannot qualify	0	-	Conservative
6	Fail	Pass	0	-	
7	Pass	Cannot qualify	0	-	
8	Cannot qualify	Fail	1	3%	Non-conservative
9	Pass	Fail	0	-	

Zones 1-3 represent a neutral result in which the same qualifying condition is met when either conditioning technique is used. 80% of the samples shown in Figure 12-4 fall within a neutral zone. This is a good indication that the DSR conditioning provides very similar results to the HTGF test conditioning.

18% of the samples fall within a conservative zone, zone 4. All of these samples would pass the apparent viscosity when the HTGF test was used for conditioning, but cannot be qualified by the apparent viscosity test when the DSR was used for conditioning. This is a conservative result, but these grouts could still be qualified using the flow cone measurement in the HTGF test.

Only 3% of the samples are in a non-conservative zone, zone 8. In this case, the grout would fail the apparent viscosity test when using the HTGF test for conditioning, but it could not be qualified when using the DSR for conditioning. The sample that fell within this zone was very close to failing under both conditions, but the apparent viscosity was slightly less than 1,500 mPa*s when the DSR was used for conditioning.

Zones 6 and 9 are the least desirable zones. These zones would result in a pass under one conditioning technique, and a fail under the other conditioning technique. None of the samples fell within either of these zones.

Overall, it seems that the DSR can be used to simulate the conditioning process imposed on the grout by the HTGF test. This is a somewhat conservative technique.

9.11 High Shear Mixer Conditioning

The high shear mixer described in section 5.2 was investigated for its potential to replace the conditioning aspect of the HTGF test. The water bath on the high shear mixer was used to hold the sample temperature at approximately 100°F, based on the results measured during the HTGF test. The procedure used to condition the grout over the period of one hour in the high shear mixer was as follows:

1. Mix grout according to the mix procedure in high shear mixer with water bath set to 100°F. The grout materials are stored at room temperature.
2. Run low speed agitator paddle at 35 RPM continuously for one hour.
3. One minute before sampling, run high speed agitator at 3,500 RPM.

4. Collect sample every 15 minutes for flow cone and mud balance testing.

A comparison of the flow cone time measured using the high shear mixer for grout conditioning versus that measured during the HTGF test is shown in Figure 12-5.

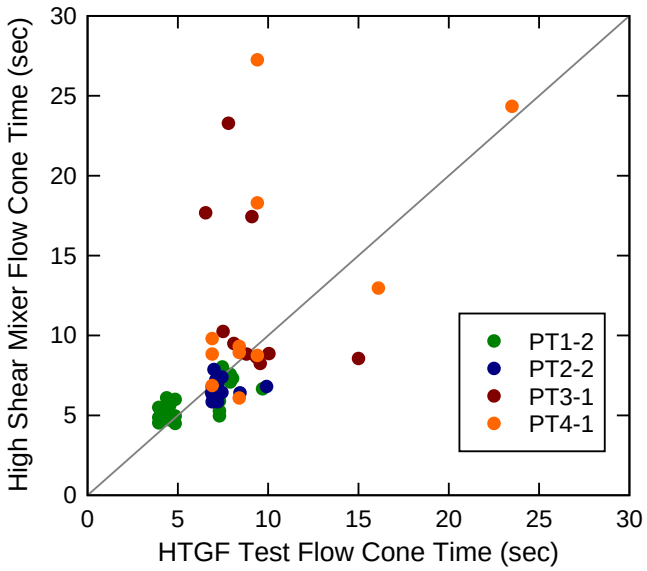

Figure 12-5. Plot of flow cone time measured where high shear mixer was used for grout conditioning versus flow cone time measured during HTGF test.

Grout PT4-1 was tested after the manufacturer's expiration date when the high shear mixer simulated conditioning tests were run. This may explain the higher flow cone times measured during the simulated conditioning tests as opposed to the actual HTGF test. Grout PT3-1 exhibited a large degree of shear-thinning and thixotropy. The amount of time that passed between collecting a sample and running a flow cone test had a significant effect on the measured flow cone time. This provides an adequate basis to disregard the data collected for grouts PT3-1 and PT4-1. Figure 12-6 contains the same results shown in Figure 12-5 for grouts PT1-2 and PT2-2 only.

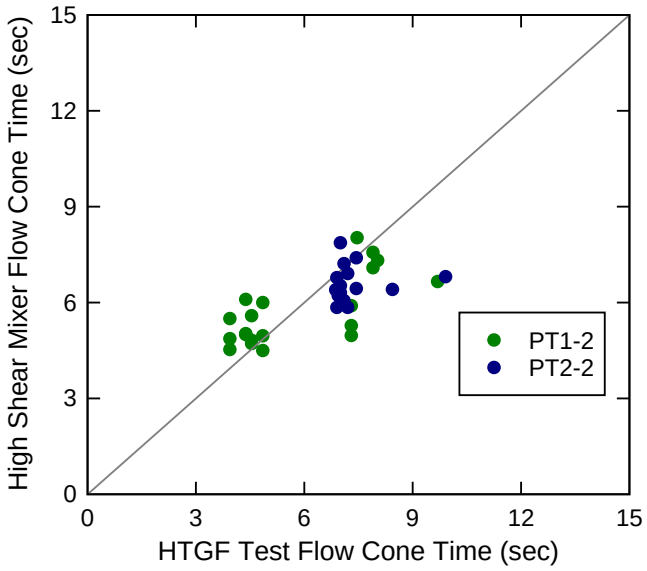

Figure 12-6. Selected data from plot of flow cone time measured where high shear mixer was used for grout conditioning versus flow cone time measured during HTGF test.

Based on the results presented in Figure 12-6, the high shear mixer can be used to replicate the conditioning process imposed on the grout by the HTGF test for grouts with low flow cone times. Similar flow cone times are measured where the high shear mixer is used to condition the grout and during the HTGF test. However, very little data were recorded for flow cone times above about 10 seconds. Grouts PT1-2 and PT2-2 exhibited very low flow cones during the entire 60-minute simulated conditioning period and during the HTGF test's 60-minute recirculation period. Recommended criteria for qualifying PT grouts using the high shear mixer and flow cone are given in Table 12-2. These are based on the limited data presented here.

Table 12-2. Recommended criteria for qualifying grouts using high shear mixer and flow cone.

Flow cone result	Qualifying condition
Flow cone time ≤ 10 sec	Grout passes.
Flow cone time > 10 sec	Cannot qualify. Run HTGF test or apparent viscosity test.

In addition to flow cone tests, mud balance tests were run on each sample during the high shear mixer simulated conditioning tests. A comparison of the mud balance

densities measured using the high shear mixer for grout conditioning versus those measured during the HTGF test is shown in Figure 12-7.

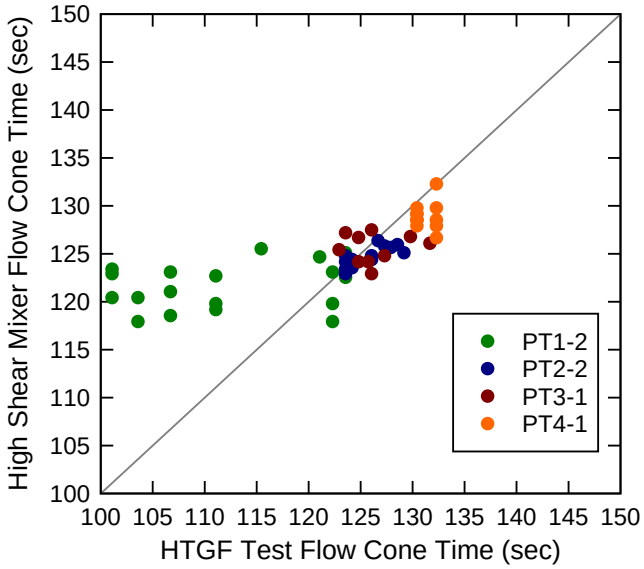

Figure 12-7. Plot of mud balance value measured where high shear mixer was used for grout conditioning versus mud balance value measured during HTGF test.

With the exception of grout PT1-2, all of the grouts exhibit a fairly similar mud balance value where the high shear mixer was used to condition the grout as they do during the actual HTGF test. However, the significant drop in density in grout PT1-2 over the course of the one hour conditioning period during the HTGF test was not measured where the high shear mixer was used. This indicates that, even though this conditioning technique can be used to assess the grout fluidity, it does not replicate the foaming issues in grout PT1-2 discovered during the HTGF test.

CHAPTER 13
SUMMARY AND CONCLUSIONS

The goal of this project was to develop a replacement for the HTGF test that made use of a DSR. Initially, currently available DSR test methods were reviewed. These included the flow curve test, the stress growth test, and the oscillatory time sweep test. None of these tests were found to be adequate to assess the rheological properties of the PT grouts. Instead, the apparent viscosity test was developed to simulate the flow cone measurement in the HTGF test. The HTGF test was run twice on four different commercially available PT grouts. While running the HTGF test, the following data were recorded: flow cone time, apparent viscosity, ambient temperature, grout temperature, pumping pressure, grout flow rate, mud balance, and unit weight. Results measured during the HTGF test were used to determine an apparent viscosity limit for qualifying PT grouts. In addition, two techniques were investigated to simulate the conditioning process of the HTGF test. These include the high shear mixer and the DSR. Several conclusions were made after conducting research.

The cup and helical ribbon geometry is the best geometry for testing PT grouts. Two DSR geometries were investigated to assess the fluidity of the PT grouts. The primary advantage of the parallel plates is that they allow variable gap spacing to simulate the spacing of aggregate in concrete. The PT grouts are not used with aggregate, so simulating this spacing is not important. The serrated plates require an adjustment to the test procedure based on the maximum particle size while the cup and ribbon does not. The cup and ribbon allows for longer tests than the parallel plate because sedimentation and temperature loss are not issues. Additionally, it is very difficult to load grouts with low viscosity onto the plates without them flowing off of the plates. This is not an issue with the cup and ribbon. Finally, the cup and ribbon was

calibrated using a NIST standard material that can be purchased by anyone. This allows for repeatable test results across multiple laboratories.

The currently available DSR test methods for assessing the rheological properties of plain grouts are not suitable for PT grout testing. The flow curve test was unsuitable for PT grouts because the grouts exhibited very different flow curves. The stress growth test could not be run using the cup and ribbon geometry because the ribbon caused the grout to yield before a point could be sampled. The oscillatory test could be used to assess the change in elastic stiffness of the PT grouts, but it did not provide insight into the fluid properties.

The apparent viscosity test, which was developed as a part of this research, provides a good simulation of the flow cone test at a shear rate of 50 s^{-1}. Parameters were selected for the testing shear rate and testing time that allowed for a good simulation of the flow cone test. The apparent viscosity test is useful for assessing the rheological properties of the PT grouts.

Grout PT4-1, which is currently on the FDOT QPL, failed the HTGF test when mixed at the mid-range of the manufacturer's specified water content. All other PT grouts tested passed the HTGF test.

The conditioning aspect of the HTGF test can be simulated using the high shear mixer or the DSR to determine fluidity. The conditioning process of the HTGF test revealed other issues in one of the PT grouts, however. Grout PT1-2 passed the HTGF test, but became aerated during the course of pumping. The unit weight dropped by 27% due to the entrained air. Neither of the simulated HTGF conditioning techniques were able to reproduce this problem.

When mixing commercial pre-packaged PT grouts, the entire bag must be mixed at the same time. It is unlikely that the admixtures and cement are distributed homogenously throughout the pre-packaged bags of PT grout. When a partial bag of PT grout is sampled, it is likely that the sample will contain a higher percentage of either cement or admixtures than is found in the entire bag. Thus, a partial bag sample of PT grout is not representative of the material that the manufacturer has produced.

CHAPTER 14
RECOMMENDATIONS

Two options are given as alternatives to the HTGF test. The first option makes use of the DSR while the second option makes use of the flow cone. Additionally, a full-scale simulation test similar to the HTGF test should be run in the future. The HTGF test's conditioning process revealed foaming issues in grout PT1-2. These issues were not observed during mixing using the blender or the high shear mixer.

In order to run the DSR alternative to the HTGF test, mix a full bag of PT grout using a high shear mixer with water bath set water bath to 100°F. The mixer must impose a shear rate comparable to a colloidal mixer. Store the grout materials and water at room temperature. Load a sample of grout into the DSR using the calibrated cup and ribbon geometry. First subject the grout to a shear rate of 165 s^{-1} for 30 seconds. Next subject the grout to a shear rate of 50 s^{-1} for a period of 60 minutes, sampling every 1 second. Make note of the maximum apparent viscosity. Qualify the grout using the conditions in Table 14-1.

Table 14-1. Recommended criteria for qualifying grouts using apparent viscosity test.

Apparent viscosity result	Qualifying condition
Apparent viscosity ≤ 750 mPa*s	Grout passes.
750 mPa*s < *Apparent viscosity* ≤ 1,500 mPa*s	Cannot qualify with apparent viscosity test. Run HTGF test.
Apparent viscosity > 1,500 mPa*s	Grout fails.

In order to use the flow cone to run an alternative HTGF test, mix a full bag of PT grout using a high shear mixer with water bath set water bath to 100°F. The mixer must impose a shear rate comparable to a colloidal mixer. Store the grout materials and water at room temperature. After mixing, run the low speed agitator paddle on the high shear mixer at 35 RPM continuously for a period of 60 minutes. Collect a sample every

15 minutes and run the flow cone test. One minute before sampling, run the high speed agitator at 3,500 RPM. Qualify the grout using the conditions in Table 14-2.

Table 14-2. Recommended criteria for qualifying grouts using high shear mixer and flow cone.

Flow cone result	Qualifying condition
Flow cone time ≤ 10 sec	Grout passes.
Flow cone time > 10 sec	Cannot qualify. Run HTGF test or apparent viscosity test.

LIST OF REFERENCES

ACI. (2010). "ACI Concrete Terminology.".

Ait-Kadi, A., Marchal, P., Choplin, L., Chrissemant, A., and Bousmina, M. (2002). "Quantitative analysis of mixer-type rheometers using the couette analogy." *Can.J.Chem.Eng.,* 80(6), 1166-1174.

Al Martini, S., and Nehdi, M. (2009). "Coupled effects of time and high temperature on rheological properties of cement pastes incorporating various superplasticizers." *J.Mater.Civ.Eng.,* 21(8), 392-401.

Amziane, S., and Ferraris, C. F. (2007). "Cementitious paste setting using rheological and pressure measurements." *ACI Mater.J.,* 104(2), 137-145.

ASTM C939. (2010). “Standard Test Method for Flow of Grout for Preplaced-Aggregate Concrete.”.

ASTM C1738. (2011). “Standard Practice for High-Shear Mixing of Hydraulic Cement Pastes.”.

ASTM D4380. (2006). “Standard Test Method for Density of Bentonitic Slurries.”.

Barnes, H. A. (2000). *A Handbook of Elementary Rheology.* The University of Wales, Aberystwyth, Dyfed, Wales.

ChemGrout. "CG-600 Colloidal Series." http://chemgrout.com/600.htm (10/8, 2012).

Chen, C., Struble, L. J., and Zhang, H. (2006). "Using dynamic rheology to measure cement-admixture interactions." *Journal of ASTM International,* 3(3).

Coussot, P. (2005). *Rheometry of pastes, suspensions, and granular materials : applications in industry and environment.* Wiley-Interscience, c2005, Hoboken, N.J.

Cullen, P. J., O'Donnell, C. P., and Houka, M. (2003). "Rotational rheometry using complex geometries - A review." *J.Texture Stud.,* 34(1), 1-20.

Dehadrai, M., Sant, G., Bentz, D., and Weiss, J. (2009). "Identifying the fluid-to-solid transition in cementitious materials at early ages using ultrasonic wave velocity and computer simulation." *Transition from Fluid to Solid: Re-examining the Behavior of Concrete at Early Ages - Technical Session at the 2009 ACI Spring Conference, March 15, 2009 - March 19,* American Concrete Institute, San Antonio, TX, United states, 58-67.

FDOT. (2002). "Grouting of Bridge Post-Tensioning Tendons Training Manual.".

FDOT. (2007). "Standard Specifications for Road and Bridge Construction." 938-5.

FDOT. (2013). "Standard Specifications for Road and Bridge Construction." 938.

Ferraris, C. F., and Gaidis, J. M. (1992). "Connection between the rheology of concrete and rheology of cement paste." *ACI Mater.J.,* 89(4), 388-393.

Ferraris, C. F., Geiker, M., Martys, N. S., and Muzzatti, N. (2007). "Parallel-plate rheometer calibration using oil and computer simulation." *Journal of Advanced Concrete Technology,* 5(3), 363-371.

Franck, A. "Non-standard geomtries for rheological characterization of complex fluids.".

Hackley, V. A., and Ferraris, C. F. (2001). "The Use of Nomenclature in Dispersion Science and Technology." *Rep. No. 960-03,* National Institute of Standards and Technology, Washington DC.

Khayat, K. H., and Yahia, A. (1998). "Simple Field Tests to Characterize Fluidity and Washout Resistance of Structural Cement Grout." *Cement, Concrete and Aggregates,* 20(1), 145-156.

Khayat, K. H., Yahina, A., and Duffy, P. (1999). "High-performance cement grout for post-tensioning applications." *ACI Mater.J.,* 96(4), 471-477.

Le Roy, R., and Roussel, N. (2005). "The Marsh cone as a viscometer: Theoretical analysis and practical limits." *Materials and Structures/Materiaux Et Constructions,* 38(275), 25-30.

Nguyen, V. H., Remond, S., and Gallias, J. (2011). "Influence of cement grouts composition on the rheological behaviour." *Cem.Concr.Res.,* 41(3), 292-300.

Nguyen, V. H., Remond, S., Gallias, J., Bigas, J. P., and Muller, P. (2006). "Flow of Herschel-Bulkley fluids through the Marsh cone." *J.Non Newtonian Fluid Mech.,* 139(1-2), 128-134.

Petit, J., Wirquin, E., and Khayat, K. H. (2010). "Effect of temperature on the rheology of flowable mortars." *Cement and Concrete Composites,* 32(1), 43-53.

Post-Tensioning Institute. (2012). "Specification for Grouting of Post-Tensioned Structures." USA.

Rosquoet, F., Alexis, A., Khelidj, A., and Phelipot, A. (2003). "Experimental study of cement grout: Rheological behavior and sedimentation." *Cem.Concr.Res.,* 33(5), 713-722.

Roussel, N., and Le Roy, R. (2005). "The Marsh cone: A test or a rheological apparatus?" *Cem.Concr.Res.,* 35(5), 823-830.

Sant, G., Ferraris, C. F., and Weiss, J. (2008). "Rheological properties of cement pastes: A discussion of structure formation and mechanical property development." *Cem.Concr.Res.,* 38(11), 1286-1296.

Schultz, M. A., and Struble, L. J. (1993). "Use of oscillatory shear to study flow behavior of fresh cement paste." *Cem.Concr.Res.,* 23(2), 273-282.

Struble, L. J., and Lei, W. (1995). "Rheological changes associated with setting of cement paste." *Adv.Cem.Based Mater.,* 2(6), 224-230.

Yahia, A., and Khayat, K. H. (2003). "Applicability of rheological models to high-performance grouts containing supplementary cementitious materials and viscosity enhancing admixture." *Materials and Structures/Materiaux Et Constructions,* 36(260), 402-412.

Zhu, H., Martys, N. S., Ferraris, C., and Kee, D. D. (2010). "A numerical study of the flow of Bingham-like fluids in two-dimensional vane and cylinder rheometers using a smoothed particle hydrodynamics (SPH) based method." *J.Non Newtonian Fluid Mech.,* 165(7-8), 362-375.

BIOGRAPHICAL SKETCH

Alexander Piper completed his B.S. degree in civil engineering at Rose-Hulman Institute of Technology in Terre Haute, Indiana in May of 2010. He earned his M.S. in civil engineering with a specialization in structural engineering at the University of Florida in December of 2012. Alex has completed internships at JMC Communities in St. Petersburg, FL and the US Army Corps of Engineers in Jamestown, KY. He also passed the fundamentals of engineering (FE) exam in 2010.